

# Recent Advances in 3D Printing of Biomedical Sensing Devices

*Md. Azahar Ali, Chunshan Hu, Eric A. Yttri, and Rahul Panat\**

Additive manufacturing, also called 3D printing, is a rapidly evolving technique that allows for the fabrication of functional materials with complex architectures, controlled microstructures, and material combinations. This capability has influenced the field of biomedical sensing devices by enabling the trends of device miniaturization, customization, and elasticity (i.e., having mechanical properties that match with the biological tissue). In this paper, the current state-of-the-art knowledge of biomedical sensors with the unique and unusual properties enabled by 3D printing is reviewed. The review encompasses clinically important areas involving the quantification of biomarkers (neurotransmitters, metabolites, and proteins), soft and implantable sensors, microfluidic biosensors, and wearable haptic sensors. In addition, the rapid sensing of pathogens and pathogen biomarkers enabled by 3D printing, an area of significant interest considering the recent worldwide pandemic caused by the novel coronavirus, is also discussed. It is also described how 3D printing enables critical sensor advantages including lower limit-of-detection, sensitivity, greater sensing range, and the ability for point-of-care diagnostics. Further, manufacturing itself benefits from 3D printing via rapid prototyping, improved resolution, and lower cost. This review provides researchers in academia and industry a comprehensive summary of the novel possibilities opened by the progress in 3D printing technology for a variety of biomedical applications.

## 1. Introduction

Sensors that capture biological signals from the human body have revolutionized the diagnosis and treatment of diseases and led to a dramatic improvement in the quality of human life. The area of biomedical sensors has evolved rapidly since their first implementation in cardiac pacemakers in the 1950s,<sup>[1]</sup> providing vital in vivo and in vitro monitoring of biological signals across a broad range of applications. In addition, their cost

has been reduced via advances in fabrication, and they are often miniaturized and multiplexed with several sensing modalities consolidated onto a single device.<sup>[2]</sup> The various categories of biomedical sensors include microelectrode-based bioelectronic probes,<sup>[3]</sup> biochemical sensors for disease and disease biomarkers,<sup>[4]</sup> haptic/tactile sensors,<sup>[5]</sup> and microfluidic devices for on-chip field diagnostics.<sup>[6]</sup>


The evolving sophistication of biomedical sensors has almost always been triggered by the breakthroughs in nano/micro/microscale device manufacturing methods. With this in mind, we note three key trends in the evolution of biomedical sensors over the last several decades: miniaturization, elasticity, and customization. The first trend is an ever-increasing miniaturization of the electronic elements of the sensor; both for microprocessors<sup>[7]</sup> and for electronic packaging.<sup>[8]</sup> This trend, primarily due to manufacturing advances, has led to smaller devices with improved functionality,<sup>[9]</sup> multiplexing,<sup>[10]</sup> improved implantability in biological tissue,<sup>[11]</sup> and lower power requirements. The second trend has been the fabrication of

soft electronic devices that have an elastic modulus close to that of the tissue in the human body. This trend is inspired by the large elastic modulus mismatch between the Si-based electronic devices and the human tissue—often as great as five orders of magnitude—which creates an inherent interface barrier for effective device coupling.<sup>[12]</sup> Matching the moduli provides a seamless route to capture relevant signals from the biological tissue of interest. Developments in silicone elastomers such as polydimethylsiloxane (PDMS) have helped advance this trend significantly.<sup>[13]</sup> The third trend, driven by customer needs, is the personalization of sensors for improved outcomes, and an ability for point-of-care device usage, which is highly advantageous in underserved areas. Despite the constant advancement of biomedical devices, these trends remain consistent—spurring on new and more efficient ways of manufacturing device elements.

Figure 1 illustrates the progression in the sophistication of biomedical sensors that underscore the above trends. The figure is divided according to the device fabrication method. The devices made by traditional methods such as lithography (Figure 1, left) include pacemakers, electrochemical sensors for glucose detection, and microelectrode-based sensors. These

M. A. Ali, C. Hu, R. Panat  
Department of Mechanical Engineering  
Carnegie Mellon University  
Pittsburgh, PA 15238, USA  
E-mail: rpanat@andrew.cmu.edu

E. A. Yttri  
Department of Biological Sciences  
Carnegie Mellon University  
Pittsburgh, PA 15213, USA

 The ORCID identification number(s) for the author(s) of this article can be found under <https://doi.org/10.1002/adfm.202107671>.

DOI: 10.1002/adfm.202107671

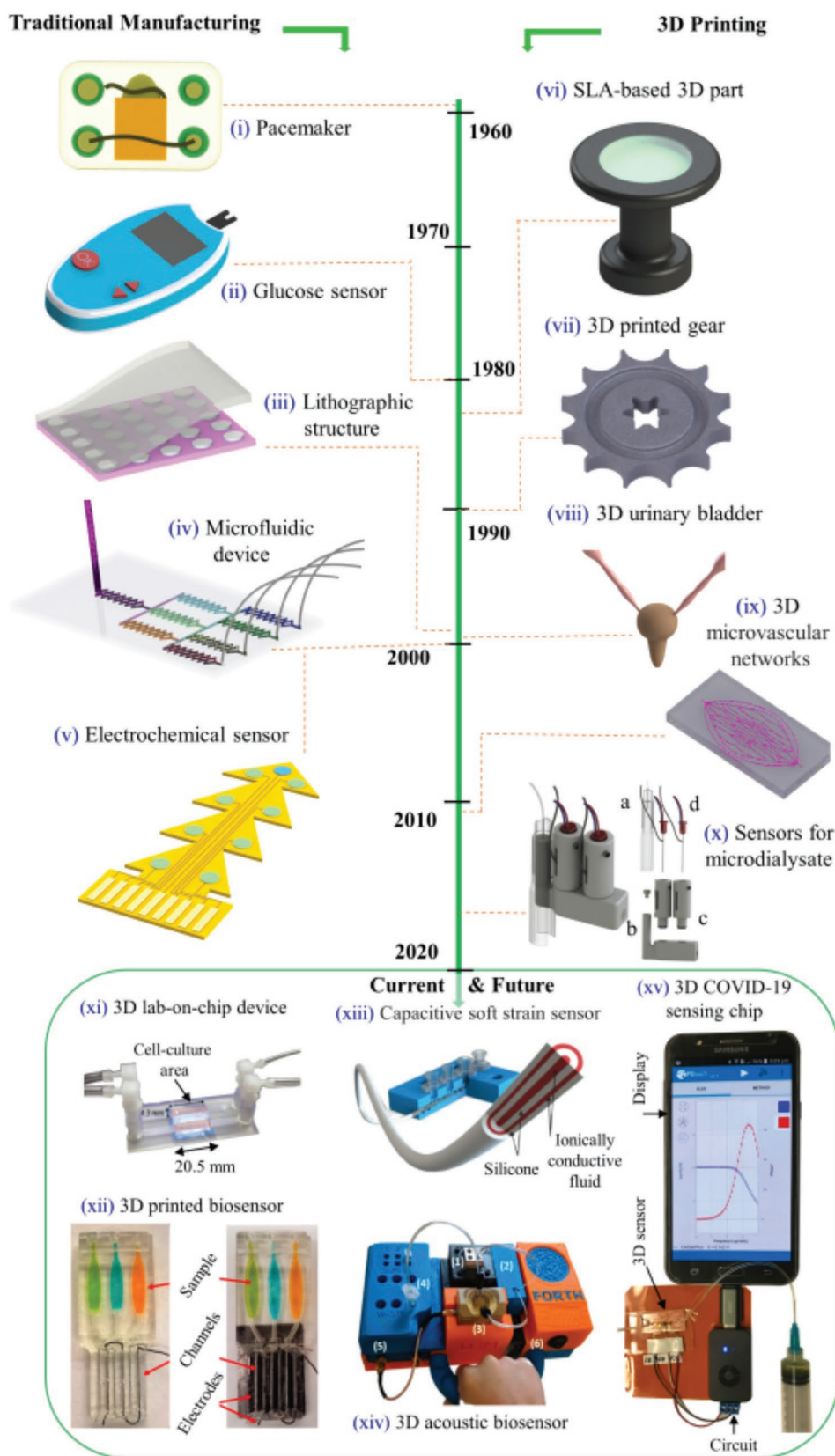


**Figure 1.** Timeline/history for the development of biomedical devices fabricated using traditional manufacturing and 3D printing. i) First implantable cardiac pacemaker invented in 1958,<sup>[1]</sup> ii) A digital glucometer based on test strip,<sup>[2]</sup> iii) schematic of microarray pattern fabrication via photolithography.<sup>[25]</sup>

methods have been around for the last half a century and have served the field well. In contrast, several emerging manufacturing methods such as Additive Manufacturing (AM), also called 3D printing, where the material is sequentially added to make parts, have been used for biomedical devices only in the last decade (Figure 1, right). In the 80s and 90s, several 3D printing methods for polymers, metals, and ceramics were developed and optimized.<sup>[14,15]</sup> These techniques later found their way into the manufacture of biomedical devices. For example, the developments in polymer stereolithography and micro-stereolithography techniques<sup>[15,16]</sup> led to the realization of custom Lab-on-a-chip biosensors based on potentiometric and chemiluminescent principles (e.g., Figure 1 xi,xii).<sup>[17–19]</sup> In recent times, developments in material jetting (a type of 3D printing technique) have led to the realization of soft and flexible biosensors with a wide range of applications (Figure 1 xiii).<sup>[20,21]</sup> In addition to biosensors, 3D printing has also led to exciting new developments in sectors such as aviation, nuclear industry, and automotive industry.<sup>[22,23]</sup> Note that the American Society for Testing and Materials (ASTM) standard classifies AM methods into seven categories, namely, a) material jetting, b) binder jetting, c) material extrusion, d) powder bed fusion, e) sheet lamination, f) directed energy deposition, and g) VAT photopolymerization.<sup>[24]</sup> The unique features of the 3D printing methods relevant to biological and physical sensors are given in **Table 1**.

In this paper, we will review the exciting developments in 3D printed biomedical sensors and highlight the prospects for this field. The intended audience includes researchers in academia as well as engineers in startups and more established companies in the biomedical and advanced manufacturing fields. The paper is arranged as follows. Section 2 highlights key functionalities and advantages of macro and micro/nanoscale 3D structures enabled by 3D printing methods as relevant to the biomedical sensors. This includes improvements in analytical sensitivity, limit-of-detection (LoD), response time, and repeatability. Section 3 summarizes the 3D printing methods as relevant to biomedical sensors. Section 4 focuses on 3D printed biosensors with different sensing modalities. These include microfluidic biosensors, soft sensors and organs-on-a-chip, and plasmonic biosensors. Section 5 talks about important advances made in biosensing due to 3D printing for the detection of pathogens; an area of high significance given the recent events related to the coronavirus pandemic. We also include the application of 3D printed physical and haptic sensors. In the last section, we discuss the future direction of 3D printed biomedical sensors that will significantly influence the advances in medical sciences.

## 2. Why 3D Printing?

Several unique features of 3D printing are fueling the trends of miniaturization, customization, and elasticity in biomedical sensors mentioned above. First, 3D printing enables different materials to be integrated with each other, which leads to the compaction of the system. For example, Kim et al.<sup>[34]</sup> used extrusion printing to integrate multiple sensing modalities on a single sensor, reducing the overall footprint of the device when compared to having separate sensors, and thereby achieving miniaturization. Second, 3D printing involves the sequential addition of material digitally controlled by computer-aided design (CAD) programs, allowing customized parts to be fabricated with high precision.<sup>[35]</sup> Third, the physical addition of material is generally not constrained by chemical compatibility which helps disparate materials to be seamlessly integrated by this method.<sup>[36]</sup> Last, 3D printing involves material deposition and curing/sintering to make the parts, which simplifies the fabrication process itself.

In the past, Clark platinum-electrodes were developed with unique geometries for continuous monitoring of oxygen concentration in cardiovascular surgery.<sup>[37]</sup> These sensors, however, were difficult to mass-produce as each sensory part was manufactured separately and assembled manually. This important issue was solved by 3D printing due to the ability to print complex geometries with multiple components as a single unit.<sup>[38]</sup> Additional examples that highlight the advantages of 3D printing are shown in **Figure 2** while categorizing them based on parts of the human body they interface with. Figure 2a shows a fully printed neural probe for brain-computer-interfaces (BCIs) where the electrode shanks are integrated with the routing on a single substrate. The fabrication of the array is achieved in two simple manufacturing steps, namely, printing and sintering.<sup>[39]</sup> The printing resolution leads to a high electrode density of recording channels ( $> 6400$  channels  $\text{cm}^{-2}$ ). Further, the 3D printing method allows an arbitrary variation in shank heights and diameters enabling the study of 3D firing patterns through the volume of the brain, which is impossible in BCIs made by traditional methods. Such customization may prove invaluable as an inroad to precision medicine in neural recording and stimulation in patients.<sup>[40]</sup> A 3D printed microfluidic device (Figure 2b) was developed for isotachopheresis with on-chip optical detection and electrophoretic separation abilities.<sup>[41]</sup> The manufacture of each device was completed in minutes using a cheap printer (\$2300) with excellent transparency that enabled the realization of the lowest cost for such sensors—illustrating the cost advantages offered by 3D printing. Figure 2d shows a 3D printed microphysiological

iv) A microfluidic device using soft-lithography replica molding.<sup>[25]</sup> v) a set of electrochemical sensors on the same substrate for in vivo biomolecule detection.<sup>[26]</sup> vi) First SLA-printed 3D part created by Chuck Hull.<sup>[27]</sup> vii) A 3D gear made by SLS method using metal powders and powder blends.<sup>[28]</sup> viii) First use of a lab-grown urinary bladder made from molded polymer for transplant surgery.<sup>[29]</sup> ix) 3D printed (omnidirectional) microvascular networks within a hydrogel reservoir using direct ink writing method.<sup>[30]</sup> x) 3D printed biosensors for online analysis of subcutaneous human microdialysate, a) a microvial, b) probe holder, c) sensor sealing holder, and d) glucose and lactate sensor probes. Reproduced with permission.<sup>[31]</sup> Copyright 2015, American Chemical Society. xi) A 3D printed lab-on-a-chip device platform for biosensing applications.<sup>[17]</sup> Reproduced with permission.<sup>[17]</sup> Copyright 2015, Wiley-VCH. xii) The 3D electrochemiluminescent detection platform for the measurement of cigarette and e-cigarette smoke extracts and polluted water samples.<sup>[19]</sup> Reproduced with permission.<sup>[19]</sup> Copyright 2017, American Chemical Society. xiii) A textile-mounted 3D capacitive fiber created for the detection of elongational strains.<sup>[20]</sup> Reproduced with permission.<sup>[20]</sup> Copyright 2020, Wiley-VCH. xiv) 3D printed acoustic biosensor for infectious disease monitoring.<sup>[32]</sup> Reproduced with permission.<sup>[32]</sup> Copyright 2019, American Chemical Society. xv) A 10 s COVID-19 test chip by enabling aerosol jet 3D nanoparticle printing.<sup>[33]</sup> Reproduced with permission.<sup>[33]</sup> Copyright 2020, Wiley-VCH.

**Table 1.** Different 3D printing methods relevant to biomedical sensor applications.

Methods*	Principle	Materials	Applications	Advantages	Disadvantages	Manufacturers
Material extrusion (Fused deposition modeling)	Nozzle prints melted filament onto a build platform followed by solidification	Acrylonitrile butadiene styrene (ABS), poly lactic acid (PLA), polycarbonate (PC) polystyrene (PS), polyamide, polyetherimide (PEI) etc.	Immunosensor, Lactate sensor <sup>[56,91]</sup>	A wide range of materials can be used, faster compared to SLA, resolution $\approx 350 \mu\text{m}$ <sup>[92]</sup>	Requires support and parts can have lower strength compared to solid polymers. <sup>[93]</sup>	Makerbot, Ultimaker Prusa
Material extrusion (Direct ink writing)	Liquid ink is extruded from a nozzle	Ceramic slurry, metal inks, graphene, carbon etc.	Metal electrodes, <sup>[71]</sup> microvascular networks <sup>[69]</sup>	Compatible with a variety of materials, including biological inks, can use multiple solidification methods <sup>[94]</sup>	To achieve small feature, ink formulation or specific process modifications are required <sup>[95]</sup>	Envision TEC 3D-Bioplotter, RepRap Prusa i3 printer
Vat photopolymerization (Stereolithography)	UV light polymerization	Photoresins, ABS, PC, polyethylene, polypropylene, nanocomposite <sup>[96]</sup>	Cellular Sensor, <sup>[97]</sup> DNA sensor, <sup>[98]</sup> Bone tissue scaffold and biomedical implants. <sup>[99]</sup>	Simple and scalable process. Ability to pattern multiple resins in same layer with strong interlayer adhesion <sup>[100]</sup>	Lower mechanical strength compared to bulk polymers, difficulty in removing uncured resins, and can print only straight layers <sup>[101]</sup>	FabPro, Form2
Vat photopolymerization (Digital light processing)	Digital projector is used to cure photoresins	Photoesins, metal powders, polymers, ceramics	Glucose sensor, <sup>[102,103]</sup> motion sensor <sup>[103]</sup>	Faster than SLA, uncured photopolymer can be reused.	Difficulty in printing large structures, <sup>[104]</sup> and difficulty in controlling precise structural shape <sup>[105]</sup>	3D PrinterPro, Fast Radius
Vat photopolymerization (Two-photon polymerization)	Two photon absorption and polymerization	Polymers, negative or positive photoresists <sup>[106]</sup>	Tissue scaffolds, <sup>[107]</sup> lab-on-CMOS sensor <sup>[108]</sup>	Sub-100 nm resolution <sup>[109]</sup>	Requires sophisticated optical circuitry and positioning stage. <sup>[51]</sup>	TOPTICA Photonics AG, Aerotech
Powder bed fusion (Selective laser sintering)	Laser source used to sinter powder particles	Metal powders, Nylon, Polyamide powders	Biomaterials, <sup>[110]</sup> pH sensors <sup>[75]</sup>	Fabrication of large parts, <sup>[111]</sup> resolution $\approx 100 \mu\text{m}$	Requires more time compared to SLA and FDM, limited accuracy of features below a millimeter, requires post-printing processes, and challenging to control porosity. <sup>[112]</sup>	Fuse 1, Sintratec
Material Jetting (Inkjet printing)	Extrusion of ink and powder liquid binding	Photo-resins, hydrogels, carbon nanotubes <sup>[113]</sup>	Bionic ear, <sup>[114]</sup> Bio-membrane <sup>[115]</sup>	Drop-on-demand, allows high-throughput cell patterning <sup>[116]</sup> and reactive ink can be printed without agglomeration <sup>[117]</sup>	Serial process, constrained by viscosity of solvents <sup>[118]</sup>	Hsusa, Ink cups, NanoDimension
Material Jetting (Aerosol Jet Printing)	Aerosolized droplets delivered by a carrier gas to deposition nozzle and focused by a sheath gas	Metal nanoparticles, polymers, carbon nanotubes, <sup>[119]</sup> graphene, MXene	Glucose sensor, <sup>[87]</sup> Protein microarray <sup>[120]</sup>	Printing in 3D without support, <sup>[52]</sup> adoptable to a wide viscosity range, <sup>[121]</sup> and high resolution of $10 \mu\text{m}$	Particle size limited to $< 500 \text{ nm}$ , over-spray <sup>[122]</sup>	Optomec, Integrated Deposition Solutions (IDS) Inc.

\*Categorization of 3D printing methods according to ASTM Standard F2792-12a<sup>[24]</sup>

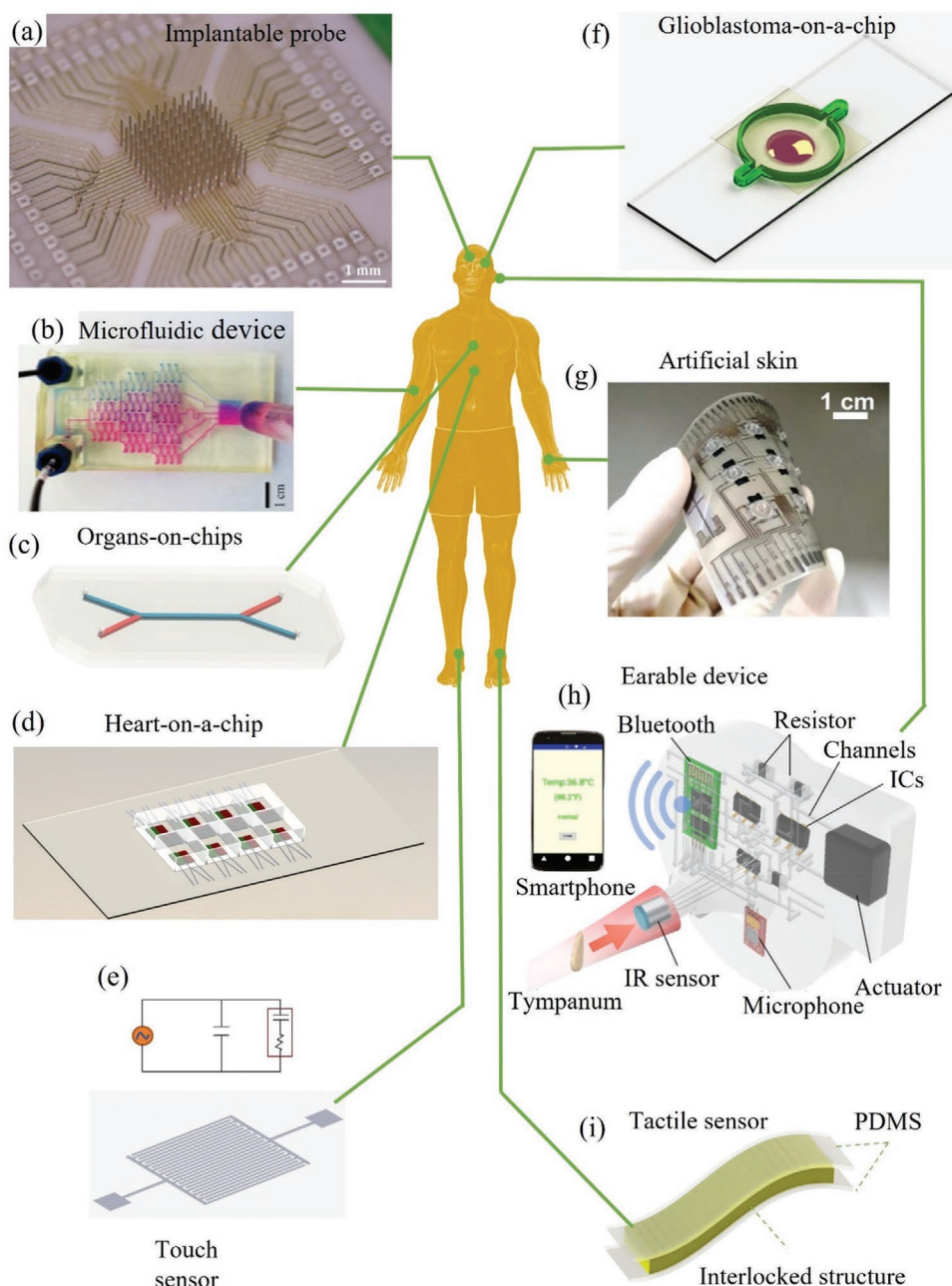


**Figure 2.** 3D printed biomedical devices that interface with various parts of the human body. a) An ultra-high-density microelectrode array for neural detection.<sup>[39]</sup> b) An optically transparent 3D microfluidic device.<sup>[41]</sup> Reproduced with permission.<sup>[41]</sup> Copyright 2014, American Chemical Society. c) Human organ-on-chip,<sup>[59]</sup> d) multimaterial microphysiological device for monitoring contractile stress of multiple laminar cardiac micro-tissues,<sup>[42]</sup> e) A printed capacitive touch sensor,<sup>[60]</sup> and f) glioblastoma-on-a-chip for drug discovery.<sup>[43]</sup> g) Artificial skin for slip force, tactile force, and temperature measurements.<sup>[21]</sup> Reproduced with permission.<sup>[21]</sup> Copyright 2014, American Chemical Society. h) 3D printed smart earable device to monitor body temperature.<sup>[44]</sup> Reproduced with permission.<sup>[44]</sup> Copyright 2017, American Chemical Society. i) A skin-attachable flexible strain sensor based on interconnected nanofibers.<sup>[61]</sup>

device (organ-on-a-chip) for the detection of contractile stress of laminar cardiac micro-tissues with multiple integrated sensors.<sup>[42]</sup> Each device contained an embedded strain sensor, and multi-layer cantilevers composed of a base layer, a tissue-guiding layer, connectors for readout, and eight independent wells using multiple material combinations such as polymers and conductive materials.<sup>[42]</sup> 3D printing enabled a rapid

multi-material system integration and allowed elasticity for seamless functioning of the sensors with the biological tissue. Such a feat would not be possible with conventional lithography due to the required process temperatures and the use of toxic chemicals, especially in the presence of biological tissue. Figure 2e shows design of an interdigitated capacitive touch sensor which was fabricated by aerosol jet printing (AJP), a

material jetting method, to achieve high sensitivity and high areal sensor density.<sup>[60]</sup> A glioblastoma-on-a-chip (Figure 2f) for drug discovery and personalized cancer treatment was developed by Yi et al.<sup>[43]</sup> This work demonstrated drug combinations associated with superior tumor killing for specific patients. 3D printing allowed a fast production of an ex vivo glioblastoma model required in testing chemotherapy drugs which are highly critical for this rapidly advancing disease.<sup>[43]</sup> Using 3D printing, an advanced artificial skin (e-skin) was manufactured by integrating three-axis tactile force and temperature sensors with fingerprint-like structure to detect the touch, slip, and friction force (Figure 2g).<sup>[21]</sup> This device represents a fully functional e-skin that imitates the softness of human skin with an integration of a staggering 45 sensors in arrays of 15 mm × 15 mm areas—and all achieved only by printing. This example highlights the trend of miniaturization and elasticity enabled by the 3D printing methods. An integrated 3D printed wearable “earable” device with an infrared sensor shown in Figure 2h was designed to be worn on the ear to detect core body temperature.<sup>[44]</sup> In order to realize personalized ear-shaped molds and circuits, they used a monolithic 3D printing process with the embedding of liquid metal microchannels. The personalization aspect of this device was clearly enabled by 3D printing. A skin attachable flexible sensor is shown in Figure 2i.<sup>[61]</sup> We note that in several 3D printed biomedical sensors, only parts of the sensor are 3D printed, requiring their assembly/attachment with non-3D printable components.<sup>[45]</sup> Active research in areas such as multi-material printing is being pursued to achieve entirely 3D printed devices with minimal process steps (also see Section 7).<sup>[46]</sup>

In addition to the exciting devices mentioned above, 3D printing also offers the possibility of making precisely fabricated 3D geometries with certain surface topographies that can lead to hierarchical architectures that are advantageous in certain circumstances. In fact, hierarchical geometries are expected to give rise to enhanced reaction kinetics and reduced reaction times, resulting in a lower LoD, rapid detection, and a large dynamic range of detection.<sup>[47,48]</sup> The AJP method was employed to create a micropillar-based hierarchical structure where sintered particles offered excellent surface topography for the attachment of nanomaterials such as graphene, resulting in the rapid detection of dopamine at sensitivities down to femtomolar concentrations.<sup>[49]</sup> Although lithography can create 3D hierarchical structures/architectures, the techniques are typically complex and more difficult to implement<sup>[50]</sup> compared to those by 3D printing methods such as two photon polymerization or 2PP<sup>[51]</sup> and AJP.<sup>[52]</sup> Additional advantages include high reproducibility, robustness, and reliability of the biosensors.<sup>[33,53]</sup> For example, AJP was employed to create high-precision microelectrode arrays for immobilization of glucose oxidase for detection of glucose<sup>[54]</sup> with a good sensitivity ( $9.9 \mu\text{A mm}^{-1}$ ) and low noise level (1.5 nA) due to spherical diffusion of targets and larger surface area.<sup>[54]</sup> A mechanically robust microfluidic device was developed for online analysis of biomarkers (glutamate, glucose, and lactate) in a microdialysis stream at a  $\mu\text{L min}^{-1}$  flow rate.<sup>[55]</sup> Another example is a 3D biosensor made of gold (Au) plated, helical stainless steel structures using selective laser melting or SLM, a powder bed fusion 3D printing technique, for the detection of DNA

hybridization with superior selectivity and a wide detection range (1–1000 nm).<sup>[56]</sup> Along the same lines, a 3D printed plasmonic sensor provided a resolution for bacterial toxin detection beyond the diffraction limit and with a sensitivity down to the size of a single molecule<sup>[57]</sup> and also an extremely high spectral sensitivity ( $>2600 \text{ nm/reflective index unit or RIU}$ ).<sup>[58]</sup>

### 3. 3D Printing Methods Relevant to Biomedical Sensors

In the previous section, we discussed the exciting advantages offered by 3D printing for bio-implants, brain-machine interfaces, and microfluidic biosensors.<sup>[48]</sup> To understand the fabrication side better, it is important to know about the 3D printing techniques used to make such devices. 3D printing methods are generally categorized as extrusion-based processes, laser-based processes (for both metal and polymer), and material jetting processes which create features at the nano, microscales. Table 1 lists various 3D printing methods (classified according to ASTM Standard F2792-12a) as relevant to biomedical sensors and devices highlighting their capabilities and applications.

In material extrusion type of 3D printing, the material is dispensed through a nozzle or an orifice. One such method, fused deposition modeling or FDM, can build 3D parts using materials such as nylon, polylactic acid (PLA), polyethylene terephthalate (PET), acrylonitrile butadiene styrene (ABS), and their blends (Figure 3a).<sup>[62]</sup> A PDMS-based microfluidic e-tongue sensor manufactured by the FDM method is shown in Figure 3b.<sup>[63]</sup> Another type of material extrusion method, direct ink writing or DIW, involves dispensing material from a nozzle, typically under a pressure (Figure 3c).<sup>[64]</sup> An implanted soft biosensor was fabricated using DIW for simultaneous epicardial recording of electrocardiography (ECG) signals from the murine heart as shown in Figure 3d.<sup>[65]</sup> In addition, the capability of introducing multiple printheads and even printhead array in DIW enables the one-step high-speed multi-material fabrication, which further enhances the possibility of mass production of highly customized biomedical devices.<sup>[66,67]</sup> Being inspired by this  $\mu\text{m}$ -resolution printing technique, several devices such as 3D periodic structures,<sup>[68]</sup> 3D microvascular networks,<sup>[69]</sup> photonic structures<sup>[70]</sup> with 3D metal electrodes,<sup>[71]</sup> and drug-delivery devices<sup>[72]</sup> have been demonstrated.

Laser-based processes use light energy to form solid shapes from precursors. Vat photopolymerization such as stereolithography or SLA (Figure 3e), digital light processing or DLP, and 2PP (Figures 3f) use polymerization of liquid resin using laser energy to form the parts. Rapid detection of bacteria was realized by an optical-fiber based probe which was manufactured using 2PP method (Figure 3g).<sup>[74]</sup> 2PP was utilized to create a set of surface-enhanced Raman spectroscopy (SERS) array structures such as a hexagonally arranged single-voxel array, a microspike array, and an array of fractal trees.<sup>[74]</sup> With a minor modification to SLA, a multi-material microstereolithography ( $\mu\text{SLA}$ ) method was recently introduced that can provide accuracy to the micron level.<sup>[23]</sup> The DLP utilizes a digital light projector for the polymerization process where micron and submicron resolution can be achieved. In the case of selective laser sintering (SLS, Figure 3h) powders

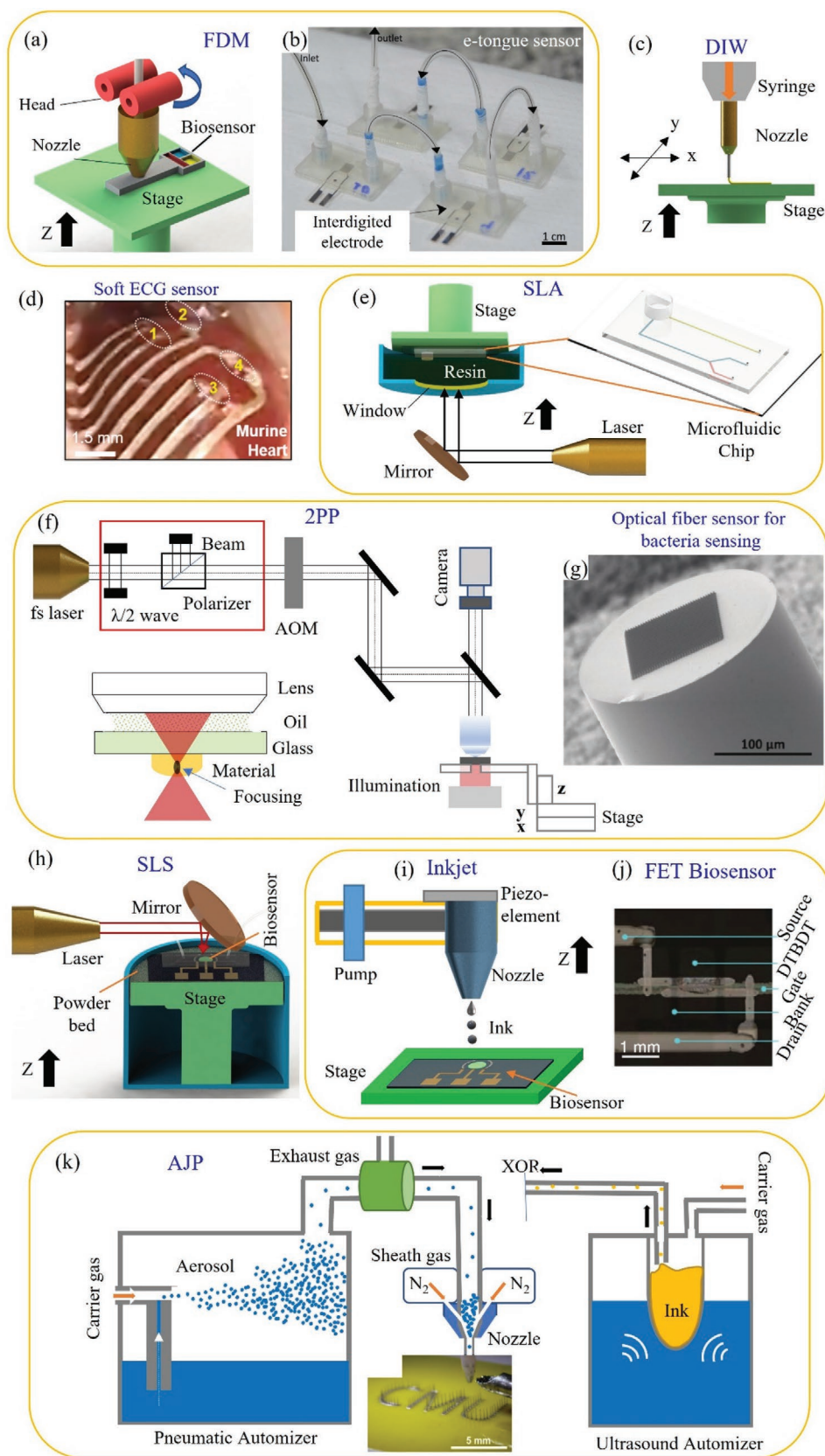


**Figure 3.** AM (also called 3D printing) methods relevant to biomedical sensors. a) Fused deposition modeling (FDM) system for printed sensors such as an electrochemical sensor for lactate sensing.<sup>[63]</sup> b) An example of biosensor (microfluidic e-tongue sensor) manufactured by FDM (image

are sequentially melted and re-solidified over a specific area per layer to create metal or polymer parts. Unlike laser polymerization, a variety of materials such as polymers, metals, ceramics, and composites could be fabricated by SLS. This material versatility gives rise to promising applications such as autoclave devices that can monitor pH during microbial shake flask cultivation.<sup>[73]</sup>

Material jetting is a non-contact layer-by-layer AM process that can deposit inks composed of nano or micro-sized particles on various substrates. Like other 3D printing methods, material jetting is also a mask-less process controlled by CAD programs wherein the materials being jetted can be readily changed at the click of a button.<sup>[77]</sup> Compared to other AM processes,<sup>[78]</sup> material jetting offers higher dimensional accuracy of printing and the ability to print at an incline or on a curved surface. This method allows microscale interconnects to be printed that helps with the integration of sensors and conformal biosensors,<sup>[79]</sup> aiding in the miniaturization of device circuits.<sup>[80]</sup> Jetting methods are being developed to create electronic circuits directly on a soft stretchable substrate with low elastic modulus<sup>[81]</sup> that matches that of the human body, thus helping with the trend of ‘elasticity’ mentioned before. Note that a large number of micro/nanoparticle (NP)-based materials can be dispersed into a solution, and used as building blocks via material jetting,<sup>[82]</sup> opening an immense material design space for sensors and devices. Material jetting can also be used to fabricate different microscale geometries such as microlattices, spirals, pillars/needles, and 3D interconnects that are difficult, if not impossible to make by conventional lithographic methods.<sup>[52,83]</sup> Amongst these methods, inkjet printing (IJP) creates circuits with feature sizes down to 50–100  $\mu\text{m}$  (Figure 3i). An organic thin-film transistor (OTFT) biosensor was fabricated by IJP with high carrier mobility (Figure 3j).<sup>[76]</sup> The IJP is also capable of printing live cells. Applications such as a 3D bionic ear consisting of cell-seeded hydrogels, silver NPs in a flexible polymer, a stretchable, capacitive-based, physical sodium chloride sensing device,<sup>[84]</sup> microelectrodes,<sup>[85]</sup> and a flexible thermistor<sup>[86]</sup> have been demonstrated by IJP. AJP is a recent 3D printing method that further improves the minimum printed feature size to  $\approx 10 \mu\text{m}$ , which is about 1/10th the size of nozzle, thanks to a focused sheath gas beam (Figure 3k). In addition, AJP enables microscale architectures such as pillars and lattices to be fabricated without any support structures.<sup>[52]</sup> A multiplex electrochemical sensor (six sensors) platform was created for glucose sensing by using AJP.<sup>[87]</sup> Other applications such as epidermal electronics,<sup>[81]</sup> terahertz metamaterials,<sup>[88]</sup> cell patterning with high porosity,<sup>[89]</sup> wearable bandage strain sensor,<sup>[90]</sup> and brain-computer interfaces<sup>[39]</sup> have been demonstrated using AJP.

## 4. 3D Printed Biomedical Sensor Devices

The range of 3D printed biomedical sensors is quite broad. As such, we will use their sensing capabilities to focus further discussion. First, microfluidic biosensors are well-suited for the manipulation and analysis of various cells, biomolecules, and other particles, which is enhanced by the customization offered by 3D printing. Second, gel-based soft conductive biosensing elements mimicking human sensing organs can be conveniently fabricated by methods such as extrusion-based 3D printing. These sensors provide a platform for organs-on-a-chip constructs used for personalized medicine. Both device types provide an in vitro space that mimics the biological environment and allows an easy approach to observe and analyze the biomedical reactions in a controlled and automated way with minimal sample volume and reasonable cost. We conclude with a summary of the array of other biomedical sensor types, emphasizing throughout what key facets 3D printing has enabled.

### 4.1. 3D Printed Microfluidic Biosensors

Microfluidic devices facilitate a controlled introduction of biomolecules in a wet environment, a feature that is highly convenient for biosensing.<sup>[123]</sup> Fabrication of microfluidic components (channels, valves, mixers, pumps, etc.) has been done by micromachining, micro-molding, and soft lithography, with many of the processes requiring expensive cleanroom facilities and optical masks. These processes have difficulty creating the necessary geometries with a minimum number of steps and suffer from issues such as delamination resulting in fluid leakage and an inability to create integrated subparts such as valves with the main device. 3D printing of soft polymers has been introduced as an alternative low-cost fabrication approach to solving these issues. In doing so, a variety of fluidic structures with complex geometries can easily be manufactured such as channels, mixers, and actuators.

A complex microfluidic biosensor was manufactured by SLA for smartphone-based colorimetric quantification of urinary proteins.<sup>[124]</sup> To do so, multiple functional elements were integrated into the same device via 3D printing, such as a torque-actuated pump, a rotary valve, and a pushing valve. This allowed automatic operation without any off-chip bulky equipment. The resulting device exhibited an excellent LoD of  $8.5 \mu\text{g mL}^{-1}$ , which is lower by more than two orders of magnitude compared to other methods ( $0.1 \text{ mg mL}^{-1}$ ) and had a detection range of 0.025 to  $6.0 \text{ mg mL}^{-1}$ . In another work, a low-cost, automated 3D printing process was developed for microfluidic components such as 3D valves and pumps for

reproduced with permission).<sup>[63]</sup> Copyright 2017, Elsevier. c) Schematic representation of direct ink write (DIW) 3D printer.<sup>[65]</sup> d) A picture of implanted soft biosensor used for simultaneous epicardial recording of ECG signal from murine.<sup>[65]</sup> e) SLA-based 3D printing wherein the manufacture of a microfluidic device is taken for demonstration.<sup>[23]</sup> f) Set up of a two photon polarization (2PP) with associated optical circuitry.<sup>[73]</sup> g) An optical fiber based probe manufactured by 2PP and used for rapid detection of bacteria.<sup>[74]</sup> Image reproduced with permission.<sup>[74]</sup> Copyright 2020, Wiley-VCH. h) SLS-based 3D printer used to fabricate microfluidic electrochemical sensors.<sup>[75]</sup> i) An inkjet printer,<sup>[76]</sup> and j) A photograph of OTFT biosensor fabricated by inkjet printer.<sup>[76]</sup> Image reproduced with permission.<sup>[76]</sup> Copyright 2015, Wiley-VCH. k) Schematic of aerosol jet 3D NP printing process with ultrasonic and pneumatic atomizers to generate aerosol droplets which are moved to the nozzle via a carries gas and focused aerodynamically to print biomedical devices such as neural probes (brain-computer interfaces).<sup>[39]</sup> The categorization of the 3D printing methods in this figure according to ASTM Standard F2792-12a is given in Table 1.



controlling the mixing and distribution of fluids.<sup>[125]</sup> Another microfluidic device was developed by integrating FDA-approved clinical microdialysis probes with needle structures for direct monitoring of tissue metabolites (glucose and lactate).<sup>[31]</sup> This biosensing device was manufactured by combining two 3D printing systems wherein one was SLA-based ultra 3sp printer having resolutions of 100  $\mu\text{m}$  in *x*- and *y*- directions and  $\approx 25\text{--}100$   $\mu\text{m}$  in *z*-direction, and another one with FDM-based Objet260 printer, having the capability of printing both hard and soft plastics. The resulting device provided fast responses of  $208 \pm 6.5\text{ s}$  and  $194 \pm 15\text{ s}$  for glucose and lactate sensing, respectively. **Figure 4a** shows a microfluidic device made by 3D printing of a nanocomposite which was used for monitoring of glutamate using electrochemical reduction principle.<sup>[126]</sup> In another work, a  $500 \times 500$   $\mu\text{m}$  microchannel was fabricated and integrated into carbon and platinum electrodes to detect the concentration of dopamine and nitric oxide (NO) (**Figure 4b**).<sup>[38]</sup> The resulting device showed significant improvement in the LoD (500 nm and 1  $\mu\text{m}$  for dopamine and NO, respectively) within the detection ranges of 25–500  $\mu\text{m}$  and 76–190  $\mu\text{m}$ . The lower LoD was primarily due to the miniaturization of the electrode enabled by 3D printing where the microchannel could constrain the analyte molecules effectively for the detection.

In addition to the biomedical sensors, 3D printing is also employed to construct acoustofluidic devices by printing ceramics such as lead zirconate titanate (PZT) or lithium niobate ( $\text{LiNbO}_3$ ), which can generate vibrations at relevant frequency ranges. Patterning and reducing the thickness of PZT substrates down to 10  $\mu\text{m}$  by conventional methods such as lapping or etching (chemical and dry) remains an open challenge due to their high surface roughness, fragility, and non-uniformity.<sup>[128]</sup> Thus, direct printing of these materials introduces a new possibility to fabricate piezo-devices such as acoustofluidic and piezoelectric transducers, and ultrasound devices. In a seminal work, a pick-and-place micro-extrusion 3D printing was used to create an acoustofluidic device containing orthogonal out-of-plane piezoelectric sensors and actuators and was used as a microfluidic device.<sup>[129]</sup> In this device, various materials such as epoxy, PDMS, silver NPs, and eutectic gallium–indium, and PZT were printed layer-by-layer to generate multiple resonant modes within 0–20 MHz frequency range.<sup>[129]</sup> The unique feature of 3D printing is realized for creating microchannels, interconnects, and embedded PZT transducers with electrodes, and anchoring and acoustic impedance matching devices in a single chip.<sup>[129]</sup> 3D printing thus shows the high customizability of microfluidic devices with a variety of structural innovations.

#### 4.2. Soft Sensors and Organs-on-a-Chip

Sensors with low elastic modulus have the capability to seamlessly interface with the biological tissue of interest. One of the ways to achieve this feat is to use hydrogel-based sensor device architectures. IJP, AJP, FDM, and DIW have been used to create microstructures consisting of hydrogels mixed with various conductive inks (metal NPs, graphene, carbon nanotubes (CNTs), and organometallic compounds) for biosensing.<sup>[130]</sup> Some of these devices are on flexible platforms where performance

under twisting, folding, and bending are of major concern. An implantable sensor was developed on a soft PDMS substrate by the direct patterning of platinum NPs, CNTs, poly(3,4-ethylenedioxythiophene) polystyrene sulfonate (PEDOT: PSS), and silicone rubber based nanocomposite ink.<sup>[131]</sup> This sensor was capable of monitoring glutamate release from an excised spinal cord segment of a Spinal Cord Injury (SCI) rat model and the results showed a LoD of 0.2  $\mu\text{M}$  with a short response time of 15 s.

AJP was used to create flexible interconnects and electronic components with feature sizes down to micrometers for conformal flow sensing in blood vessels.<sup>[132]</sup> In addition to the elasticity of the system, 3D printing allowed miniaturization, with wireless inductive coupling devices to be integrated that enabled wireless detection of cerebral aneurysm hemodynamics with a maximum readout distance of 6 cm in highly contoured and narrow human neurovascular models.<sup>[132]</sup> This measurement would be difficult, if not impossible, for sensors made using traditional lithographic techniques. IJP was used to manufacture flexible glucose sensors by printing multi-layered graphene and platinum NPs on curved surfaces of polyetheretherketone.<sup>[133]</sup> This implanted sensor was evaluated in vivo in rats, and the results showed high sensitivity and comparable data to a commercial glucometer for continuous glucose monitoring in subcutaneous tissue, even under the hypoglycemic condition.

Human organs are soft biosensors that have been evolving over several millennia. Mimicking these sensors artificially (e.g., on a chip) can allow drug development, disease modeling, and personalized medicine; and serve as an alternative to animal models for clinical studies.<sup>[134]</sup> Organs-on-chips, a technology that aims to develop artificial organs as alternative animal models have been extensively studied and proven to be effective in various biomedical fields. The technology has matured such that organs-on-chips are currently being commercialized by various companies (e.g., Emulate, Inc.).<sup>[135]</sup> These devices are fabricated by photolithographic methods, but suffer from limitations such as complex multi-step processes, poor cost-effectiveness due to cleanroom process, difficulties in surface biofunctionalization, and validation related to biocompatibility.<sup>[136]</sup> Since artificial organs rely on the self-assembly of cells to create complex-tissue, organ-level organization, and functions, 3D printing is an efficient fabricating modality that can control cell patterning at multiple layers in extracellular matrix (ECM), and positioning of micro-posts and other functional components and biomaterials on a single chip platform. In addition, 3D printing can create layer-by-layer construction of ECM, live cells, tissues, and organoids and incorporate multi-sensor elements. Several artificial sensing (or otherwise) organs including liver-on-a-chip,<sup>[137]</sup> nervous system-on-a-chip,<sup>[127]</sup> air-blood-barrier,<sup>[138]</sup> kidney organoids-on-a-chip,<sup>[139]</sup> multiple organs-on-a-chip (liver, heart, and lung),<sup>[140]</sup> heart-on-a-chip,<sup>[141]</sup> and brain organoids<sup>[142]</sup> are realized by 3D printing. With long-term time-course optical imaging capabilities, a human stomach-on-a-chip was fabricated using 3D printing to grow gastric organoids (human pluripotent stem cells) and a peristaltic pump was introduced for luminal delivery.<sup>[143]</sup> This chip lasted for long-term delivery of drugs/nutrients to investigate the gastric physiology and drug screening.<sup>[143]</sup> **Figure 4c–e**

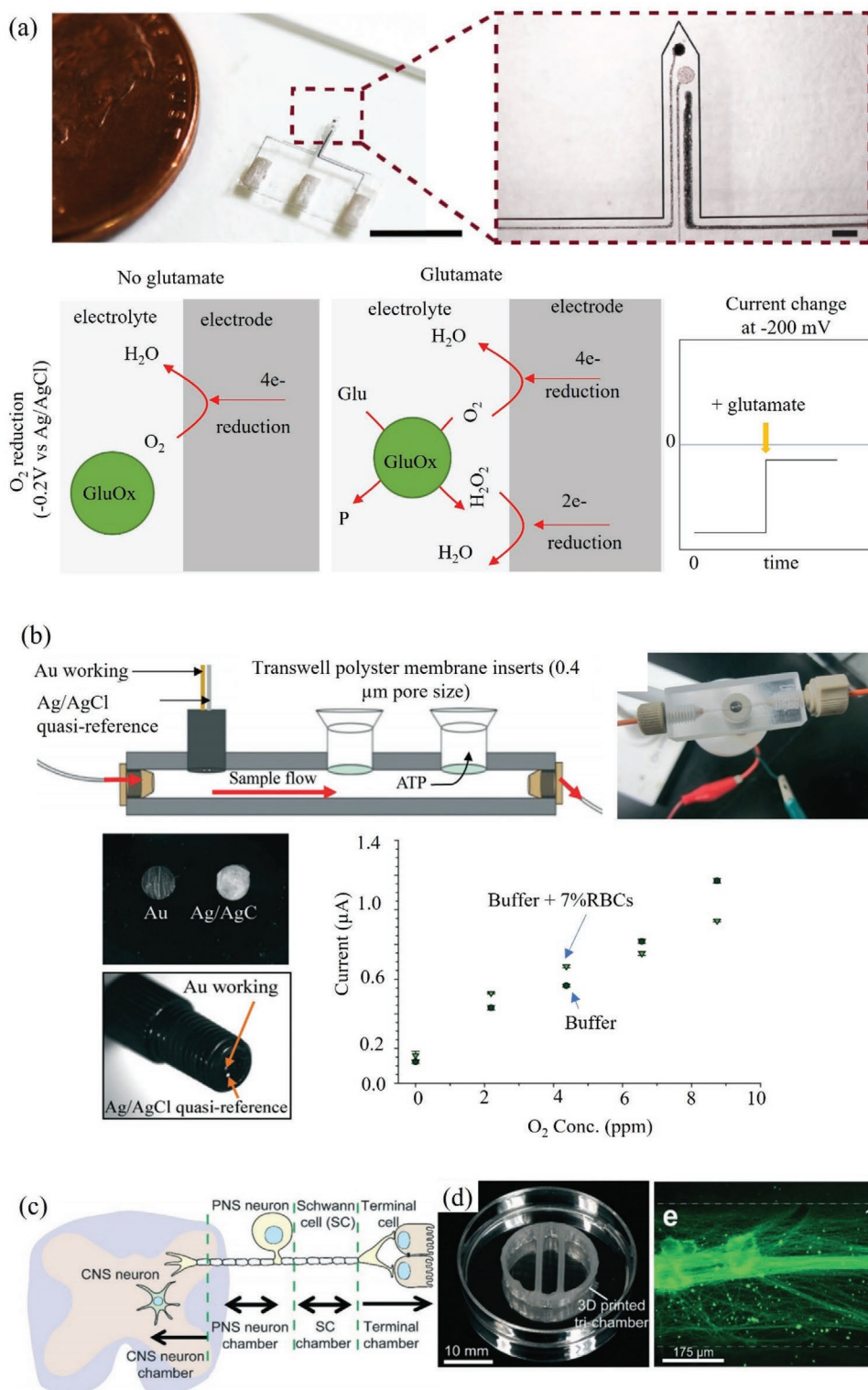


**Figure 4.** 3D printed microfluidic biosensor and organs-on-a-chip. a) 3D printed needle-type microfluidic glutamate sensor consisting of three electrodes wherein the working electrode is made of platinum NPs, CNTs, and poly(3,4-ethylenedioxythiophene) polystyrene sulfonate (PEDOT:PSS). The biochemical reaction shows the generation of electrons by oxygen ( $O_2$ ) and hydrogen peroxide ( $H_2O_2$ ) reduction in presence of glutamate oxidase enzyme.<sup>[126]</sup> Reproduced with permission.<sup>[126]</sup> Copyright 2019, Elsevier. b) A schematic and an optical image of a 3D printed modular microfluidic sensor with reusable electrodes. The micrographs show gold and silver wire secured with C-7 epoxy and a calibration plot for the detection  $O_2$  concentration (parts-per-million) in presence of buffer (HBSS) with red blood cell counts.<sup>[38]</sup> Reproduced with permission.<sup>[38]</sup> Copyright 2014, Royal Society of Chemistry. c–e) 3D printed organ-on-a-chip. The optical image shows a perpendicular assembly of microchannel and tri-chamber components of the organ-on-a-chip. The micrograph shows a single channel of superior cervical ganglia (SCG) neurons and axons in chamber 1.<sup>[127]</sup>

shows a nervous system-on-a-chip developed to study viral infection by reconstituting the critical function of neural-tissue interfaces (glial cell–axon) in the nervous system.<sup>[127]</sup> In this device, schwann cells and hippocampal neurons were observed to be refractory to axon-to-cell infection of the pseudorabies virus, indicating a bottleneck to viral transmission. These examples reveal a new direction of manufacturing for devices that mimic or even create organs with high spatial resolutions and complex geometries.

### 4.3. The Rapidly Expanding Diversity of 3D Printed Biosensors with Different Sensing Modalities

As seen before, 3D printing allows the manufacture of cheap, multifunctional, and miniaturized structures for efficient biosensors. These advantages have been utilized by sensors with various modalities described below. The sensors provide highly sensitive measures of cancer biomarkers,<sup>[144]</sup> infectious diseases,<sup>[145]</sup> metabolites,<sup>[31]</sup> neurotransmitters,<sup>[38]</sup> pathogen,<sup>[146]</sup> and other biomarkers,<sup>[147]</sup> and demonstrate specific advantages in terms of high sensitivity and specificity, low LoD, and a reconfigurable back-end that allows easy interfacing with smartphone-based readouts.<sup>[148]</sup>

Electrochemical sensors work on the principle of electrochemical transduction such as a change in impedance, current, voltage, and capacitance caused by the presence or absence of specific biomolecules.<sup>[149]</sup> Because these reaction rates depend upon the total surface area as well as the mesoscale geometry of the electrodes, 3D printing is an ideal method to greatly increase sensitivity (i.e., reduce the LoD). **Table 2** compares several electrochemical sensors made by 3D printing and conventional manufacturing methods. For prostate-specific antigen (PSA), an important disease biomarker, a 3D printed sensor showed a LoD of 0.5 pg mL<sup>-1</sup>.<sup>[150]</sup> Using conventional methods, the same sensor is only capable of detecting values in the micro-to-nanogram per milliliter range, a >3 orders of magnitude difference.<sup>[150]</sup> This 3D printed device not only provided a selective detection of serum PSA, but also brought a unique solution of mixing of reagents in microchannels during immuno-detection. In the case of dopamine, an important neurotransmitter, 3D printed multi-length-scale hierarchical electrode architecture was able to break the detection barrier described in the literature<sup>[47,48]</sup> to obtain a LoD of 0.5 aM. Lithographically produced,<sup>[151]</sup> and screen-printed carbon<sup>[152]</sup> and conducting polymer-palladium composite<sup>[153]</sup> sensors, on the other hand, showed a LoD of 128, 50, and 24 nm, respectively, for the same neurotransmitter. The superior LoD of 3D printed sensors was believed to be due to its unique hierarchical electrode architecture. Similar results are also given in Table 2 for the detection of biomolecules such as glucose and ascorbic acid. 3D printed biosensors thus provide a high sensitivity for detection of biomarkers along with high selectivity. Development of such a device has the potential to open new avenues for an early in vitro diagnosis of various diseases. Further, this progress can be combined with wearable technology that can lead to a patch-type epidermal and sweat monitoring sensor.<sup>[34]</sup>

Noble metallic nanostructures possess plasmonic properties that can be used to fabricate plasmonic biosensors for the detection of biomarkers. Surface plasmons are electromagnetic

waves propagating along a surface and evanescently decaying away from the metal-dielectric interfaces that are uniquely affected by the presence or absence of specific biomolecules due to a change of refractive index. Using direct-write printing and 2PP, many plasmonic structures can be fabricated with high quality, including Au nanostructures,<sup>[165,166]</sup> Au-containing pyramidal structures,<sup>[167]</sup> metallic structures with sub-wavelength resolution,<sup>[166]</sup> conductive Au microstructures, and Au nanocomposite.<sup>[168]</sup> Using 3D printing to create the light-emitting diode (LED) source, collimator, linear polarizer, and beam-splitter plate, a surface plasmon resonance (SPR) imaging device was fabricated, with everything attached to a smartphone.<sup>[169]</sup> This sensor provided an optimal use of the complementary metal–oxide–semiconductor (CMOS) sensor of the smartphone to give high sensitivity with excellent biological affinity. Another all 3D printed SPR biosensor was used to monitor label-free bacterial toxins with optical components, sensors, and light-guiding systems being printed.<sup>[57]</sup> Thus, 3D printing overcomes several problems with traditional bench-type plasmonic measurements while creating a portable point-of-care device for monitoring biomarkers.

Colorimetric biosensors detect a particular analyte through color changes that can be captured by optical detectors or by the naked eye.<sup>[170]</sup> Though traditional paper-fluidic colorimetric sensors have been exploited widely for biomarker monitoring, they have limited device efficacies due to their short optical path, color distribution inhomogeneity, temperature, and moisture sensitivity, and issues of spreading of the dyes from detection zones.<sup>[171]</sup> 3D printed colorimetric biosensors can solve these problems by tuning the optical path (via printing) and the active loading of the samples. With a smart phone reader, a 3D printed colorimetric sensor (**Figure 5a,b**) was demonstrated for immunoassay test of urinary proteins. This device integrates torque-actuated pump and valve, rotary valve, and push valve, via seamless 3D printing.<sup>[124]</sup>

Implantable biosensors that monitor (and react to) the bio-environments are increasingly used for applications such as supportive structures for damaged biological components, monitoring of signals in the vicinity of biological cells, and controlled drug delivery. Instead of ‘one-size-fits-all’ approach, personalized implantable sensors are increasingly favored due to improved patient outcomes. This requires the fabrication of geometrically complex shapes and compositions that need frequent on-demand changes.<sup>[172]</sup> Such sensors should also conform to the elastic modulus of the correspondent biological tissue. 3D printing is uniquely positioned to fulfill these requirements. **Figure 5c** shows a minimally invasive microneedle-based sensor with bio-inspired backward-facing curved barbs for enhanced tissue adhesion manufactured by DLP printing.<sup>[173]</sup> A fully printed chip was manufactured for counting of CD4 (i.e., CD4 positive helper T-lymphocytes or CD4<sup>+</sup> T-cells) of healthy donors and HIV-infected patients using IJP.<sup>[174]</sup> Recently, a custom gastric resident electronic (GRE) device was manufactured using multi-material 3D printing (**Figure 5d–f**) that enables the simultaneous controlled release of drugs (antimicrobial and hormonal agents).<sup>[175]</sup> This device is designed to perform the delivery of drugs orally, pass through the pylorus, and excreted out of the body. With a seamless integration of wireless module, this device has the capability for in vivo gastric residences in a porcine stomach for 36 days while also maintaining in vivo wireless communication.

**Table 2.** Comparison of 3D printed biomedical sensors with traditional sensors.

Methods	Biomarker	Sensor structures (3D and non-3D)	Detection range	LoD	Sensing capabilities and remarks
3D printing (SLA) <sup>[150]</sup>	Prostate specific antigen	3D printed channels; immunoarray	0.5 pg mL <sup>-1</sup> to 5 ng mL <sup>-1</sup>	0.5 pg mL <sup>-1</sup>	Customizability and rapid prototyping capability. Automated detection system and assay time ≈ 30 min. Accuracy comparable with ELISA and commercial devices such as Abbott Diagnostics (0.008 ng mL <sup>-1</sup> ), Roche (0.002 ng mL <sup>-1</sup> ), Beckman Coulter (0.008 ng mL <sup>-1</sup> ), and Diagnostic Products Corporation (0.04 ng mL <sup>-1</sup> )
Commercial SPR biochip <sup>[154]</sup>		Self-assembled monolayered Au	1–1000 ng mL <sup>-1</sup>	18.1 ng mL <sup>-1</sup>	Assay time ≈ 14 min. Sensing with buffer solution and human serum
Microfabrication <sup>[155]</sup>		Self-assembled monolayer Au	0–4 μg mL <sup>-1</sup>	0.2 μg mL <sup>-1</sup>	Single-use biosensor, sensing with serum samples and good sensitivity
3D Printing (AJP) <sup>[49]</sup>	Dopamine	Micropillar array electrode	100 aM–1 nM	500 aM	Low LoD ≈ 500 attomoles, breaking the barrier described in literature <sup>[47]</sup> through multi-length-scale electrode structure. Rapid prototyping capability and waste minimization due to small microfluidic volume required for testing.
3D printing (ZPP) <sup>[148]</sup>		3D carbon electrode	0.5–100 μM	10 nM	High sensitivity to multiple neurochemicals, high reproducibility, capability for both in vitro and in vivo.
Lithography <sup>[156]</sup>		Graphene	0.5–120 μM	10 nM	Good sensitivity in urine sample
Screen printed electrode <sup>[153]</sup>		Conducting polymer-Pd composite	0.1 to 200 μM	24 nM	In vitro sensing capabilities
Glassy carbon electrode <sup>[152]</sup>		Carbon paste electrode	0.5–800 μM	50 nM	Sensing capabilities with urine sample
Lithography <sup>[151]</sup>		Nano-Au electrode	4–1012 μM	128 nM	Sensing in phosphate buffered saline (PBS)
3D printing (AJP) <sup>[157]</sup>	Glucose	Polymer nanocomposite	0–10 nM	6.9 μM	Multi-materials printing, customizability and rapid prototyping. High sensitivity.
3D printing (AJP) <sup>[54]</sup>		Printed microelectrode arrays	1.7 μm–1 nM	0.45 μM	Rapid prototyping, waste minimization, and customizability. Low LoD and low noise level (1.5 nA)
3D printing (Inkjet printing) <sup>[158]</sup>		PEDOT:PSS	0.25–0.9 nM	28 μM	Rapid, fully printed, and customizable biosensor. Non-invasive, good sensitivity in saliva, stability ≈ 1 month, and response time ≈ 1 min
Electrodeposition <sup>[159]</sup>		MnO <sub>2</sub> /MWCNTs	10 μm–28 nM	10 μM	Low-potential, stable, and fast detection time
Lithography <sup>[160]</sup>		CNTs	0.05–0.3 nM	1.3 μM	Stretchable and skin attachable, continuous monitoring, stability ≈ 10 days
Screen-printing <sup>[161]</sup>		Carbon	2.5–20 nM	0.5 nM	In vitro sensing with human caucasian hepatocyte carcinoma cell line, and long-term detection of ≈ 24 h
3D printing (SLM) <sup>[162]</sup>	Ascorbic acid	Au electrode	0.1–1 nM	2.1 μM	Multi-materials printing and rapid prototyping. High sensitivity, sensing ability with real samples in vitamin C tablet, and better LoD compared to glassy carbon electrode.
Glassy carbon electrode <sup>[163]</sup>		Carbon nanoplatelets	0.1 μm–1.8 nM	1.09 μM	Sensing ability with soft drink, orange juice, and urine.
Lithography <sup>[164]</sup>		Indium tin oxide (ITO) electrode	0.058 to 0.71 nM	8.4 μM	Response time ≈ 40 s, shelf life ≈ 1.5 month

## 5. The Fast, Flexible, and Accurate Detection of Disease through 3D Printed Sensors

Finally, the rapid and accurate detection of pathogens and their biomarkers has never been more important, as shown by the recent COVID-19 pandemic.<sup>[176]</sup> In addition, infectious diseases caused by other viruses (e.g., HIV, influenza, ebola, hepatitis), parasites (malaria), and bacteria (tuberculosis),

are a major health concern throughout the world, particularly in developing countries. Biosensors that can detect the pathogens in seconds can open travel and economies of entire regions, helping with the livelihood of millions of people. Rapid and early test assay is thus an unmet need that is critical to protect public health.

To rapidly detect pathogens, electrochemical sensing with surfaces modified with nanomaterials was introduced where

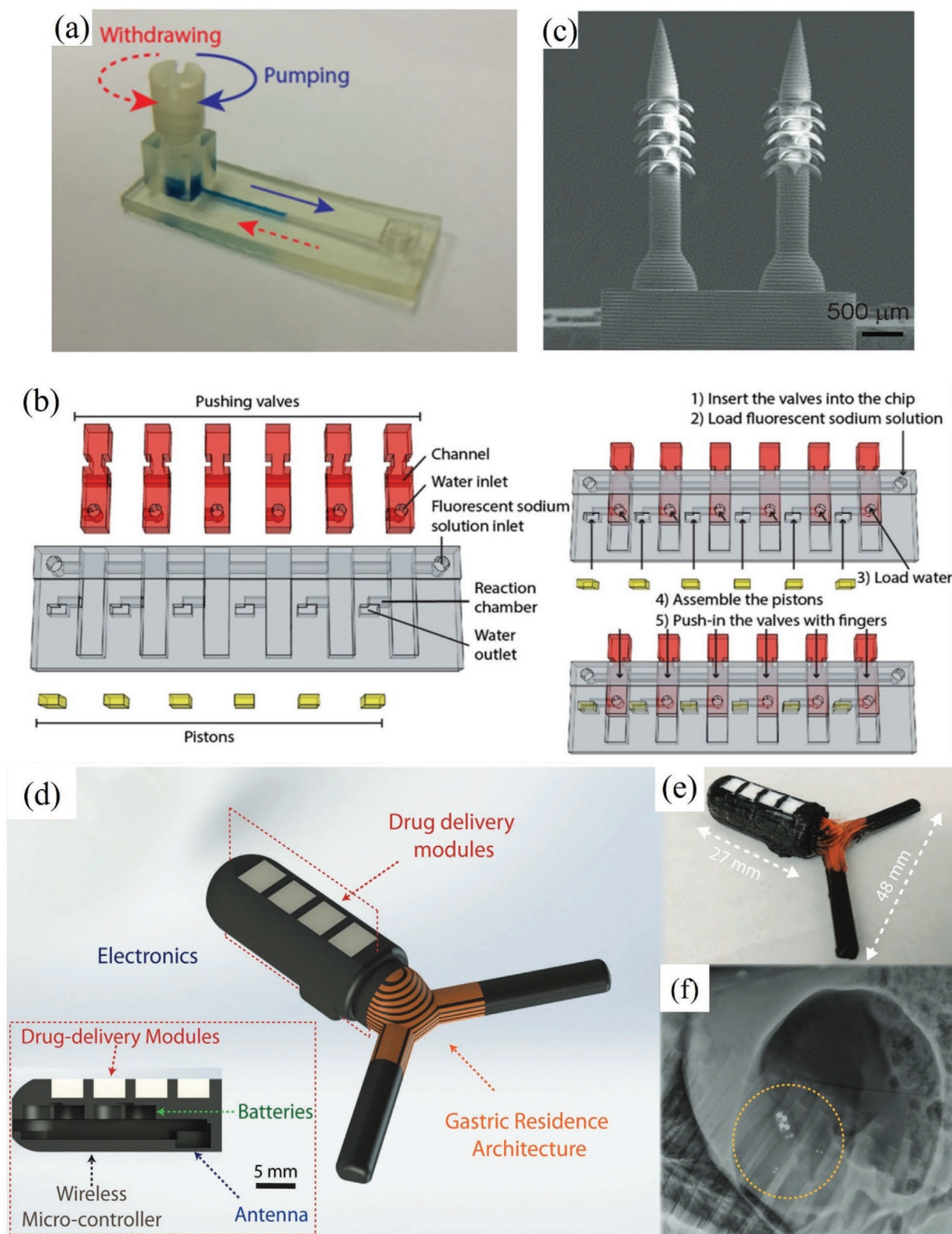


**Figure 5.** Biosensor device integration and customization via 3D printing. a) 3D printed microfluidic colorimetric sensor.<sup>[124]</sup> b) Example of using 3D printing to create custom reconfigurable components for biosensing: assembly and operation of push valves used in a microfluidic biosensor (red and yellow colors indicate valves and pistons, respectively).<sup>[124]</sup> Reproduced with permission.<sup>[124]</sup> Copyright 2016, American Chemical Society. c) 3D printed microneedles for drug delivery and biosensing.<sup>[173]</sup> Reproduced with permission.<sup>[173]</sup> Copyright 2020, Wiley-VCH. d) 3D printed GRE device<sup>[175]</sup> with a CAD layout that shows the embedded electronics for sensing and drug delivery. e) Dimension of the GRE device in (d). f) X-ray image showing the deployment of the GRE device in (d) in a porcine stomach. Reproduced with permission.<sup>[175]</sup> Copyright 2019, Wiley-VCH.

lithography was used to create an HIV detection device at an early stage of infection (3–8 weeks).<sup>[177]</sup> The same device principle was also used to detect a variety of other viral pathogens.<sup>[178]</sup> Although, the 2D planar electrode structures allow compatibility with lithographic techniques for scalable production, they have limited device performance in terms of sensitivity and response time (i.e., speed of detection). A 3D structure of the electrode would be highly beneficial to improve the reaction kinetics and hence accelerate the sensing performance. The fabrication of the 3D surfaces, however, is inherently incompatible with the planar lithographic techniques. This limitation was overcome by 3D printing in our recent work where AJP was used to create micropillars coated with reduced graphene oxide nanoflakes to sense COVID-19 antibodies within 10 s.<sup>[33]</sup> **Figure 6** shows this 3D printed device with a 10 × 10 micropillar array coated with the severe acute respiratory syndrome coronavirus 2 (SARS-CoV-2) spike S1 antigen-specific to S1 antibodies. The AJP used layer-by-layer printing of Au NPs followed by sintering at 400 °C<sup>[33]</sup> to create the working electrode of the sensor. The device was used to detect multiple antibodies such as spike S1 and receptor-binding domain (RBD) down to picomolar concentration in mere 10 s where the readout was enabled by a commercially available smartphone-based app. The device could also be regenerated 9 times and showed good reproducibility and sensitivity. Such a device can also be used to investigate the dynamics of immune response to viral infections and vaccine development with different viral strains. This 3D printing technology used a generic device set-up, and as such may be able to detect other pathogens and their biomarkers.

Other examples of the use of 3D printing for pathogen detection include the isolation and detection of influenza virus using a 3D printed microfluidic device.<sup>[179]</sup> In this work, paramagnetic beads were conjugated by glycan and labeled by quantum dots for isolation, followed by their attachment to hemagglutinin. This system was then used to effectively detect the influenza virus via differential pulse voltammetry. In a recent work, low-cost open-source electronics were integrated with 3D printing to develop a portable diagnostic platform for the detection of malaria.<sup>[180]</sup> A microfluidic magnetic pre-concentrator was manufactured via 3D printing without the need for any assembly and used to detect bacterial pathogens *Escherichia coli* (O157:H7, a pathogen that causes hemorrhagic colitis and hemorrhagic uremic syndrome by contaminating foods) using antibody-conjugated magnetic NPs.<sup>[181]</sup> This device improved the LoD, while also enabling miniaturization where a small volume of the affected fluid (blood) could be used to detect pathogens. A 3D printed acoustic wave sensor integrated with smartphone for convenient readout was developed for nucleic acid-based detection of *Salmonella* cells in biofluids such as whole blood, saliva, and nasal swab.<sup>[32]</sup> The advantages of this device were short sample-to-answer analysis time (within 30 min), a low LoD of 4 × 10<sup>3</sup> CFU (colony forming unit) mL<sup>-1</sup>, and user-friendliness and affordability to access in underdeveloped areas. As the world comes to grips with increasing numbers of potentially catastrophic diseases, the accuracy and ease of detection delivered by 3D printed sensors becomes more important than ever.

## 6. 3D Printed Physical Sensors for Monitoring of Human Health

Physical or mechanical biosensors convert mechanical signals from the human body into electrical signals and form an important category for healthcare monitoring devices. A specific requirement to have a good sensitivity for such sensors in capturing the body signals is that they need to have an elastic modulus comparable to that of the human body, that is, have the quality of ‘elasticity’ described in Section 1. Several types of tactile sensors (i.e., sensors that measure information arising from physical interaction with the environment) fall under this category and are used as wearable biomonitors, human-machine interfaces, and biotic–abiotic interfaces.<sup>[182]</sup> **Figure 7** shows several physical sensors where 3D printing has played a central role in enabling their elasticity, and hence their functionality. **Figure 7a,b** shows a 3D printed porous pressure-sensitive rubber (PSR) sensor and strain gauge for wearable human-machine interfaces.<sup>[11]</sup> In addition to monitoring human motion, the sensor can also be used by humans to interface with a robot. We note that the sensitivity of the pressure-based tactile sensor is one of the most important factors in mimicking the human skin and achieving a precise capture of human motion.<sup>[11]</sup> A multifunctional electronic skin that detects body temperature and pressure is shown in **Figure 7c**.<sup>[183]</sup> This is an example where multiple sensing modalities have been integrated into a single device via 3D printing to achieve miniaturization and elasticity. In another example, 3D printing was used to create a multi-sensor e-skin to mimic the human somatosensory system (**Figure 7d**).<sup>[184]</sup> This sensor was utilized for real-time sensing of temperature (**Figure 7e**), in-plane strain, humidity, light, magnetic field, pressure, and proximity simultaneously.<sup>[184]</sup> To detect human movements (radial pulse, bending, and finger pressing), a tactile sensor was demonstrated under conditions through a combination of composite ink optimization, 3D imaging, and multimaterial printing (**Figure 7f**).<sup>[5a]</sup>

The examples of 3D printed physical sensors illustrated in **Figure 7** form only a small subset of the current state-of-the-art in this field. 3D printing was used to create a strain sensor using carbon resistive ink within a highly conformal and extensible elastomeric matrix where the sensor geometry was controlled by maintaining print path and filament cross-section.<sup>[186]</sup> Recently, a highly flexible, wearable bandage-based strain sensor was 3D printed and used for home healthcare monitoring by combining AJ printer and laser sintering.<sup>[90]</sup> The laser sintering could locally sinter the conducting metal with minimal damage to the underlying flexible substrate.

Haptic sensors are computer-controlled electromechanical interfaces that give kinesthetic or tactile feedback to the users. In the past, prosthetic systems with haptic feedback were known to be obtrusive and bulky.<sup>[187]</sup> This issue has been addressed by 3D printing in several recent developments. 3D printed fabric-based haptic gloves and soft robotic grippers were manufactured by integrating an array of pneumatic finger actuators and flexible sensors.<sup>[188]</sup> The sensorized gripper could pick and hold objects with a wide range of weight from 50 to 1100g while the haptic actuator was capable of producing forces up to 2.1 N, which was more than the minimum force of 1.5 N required

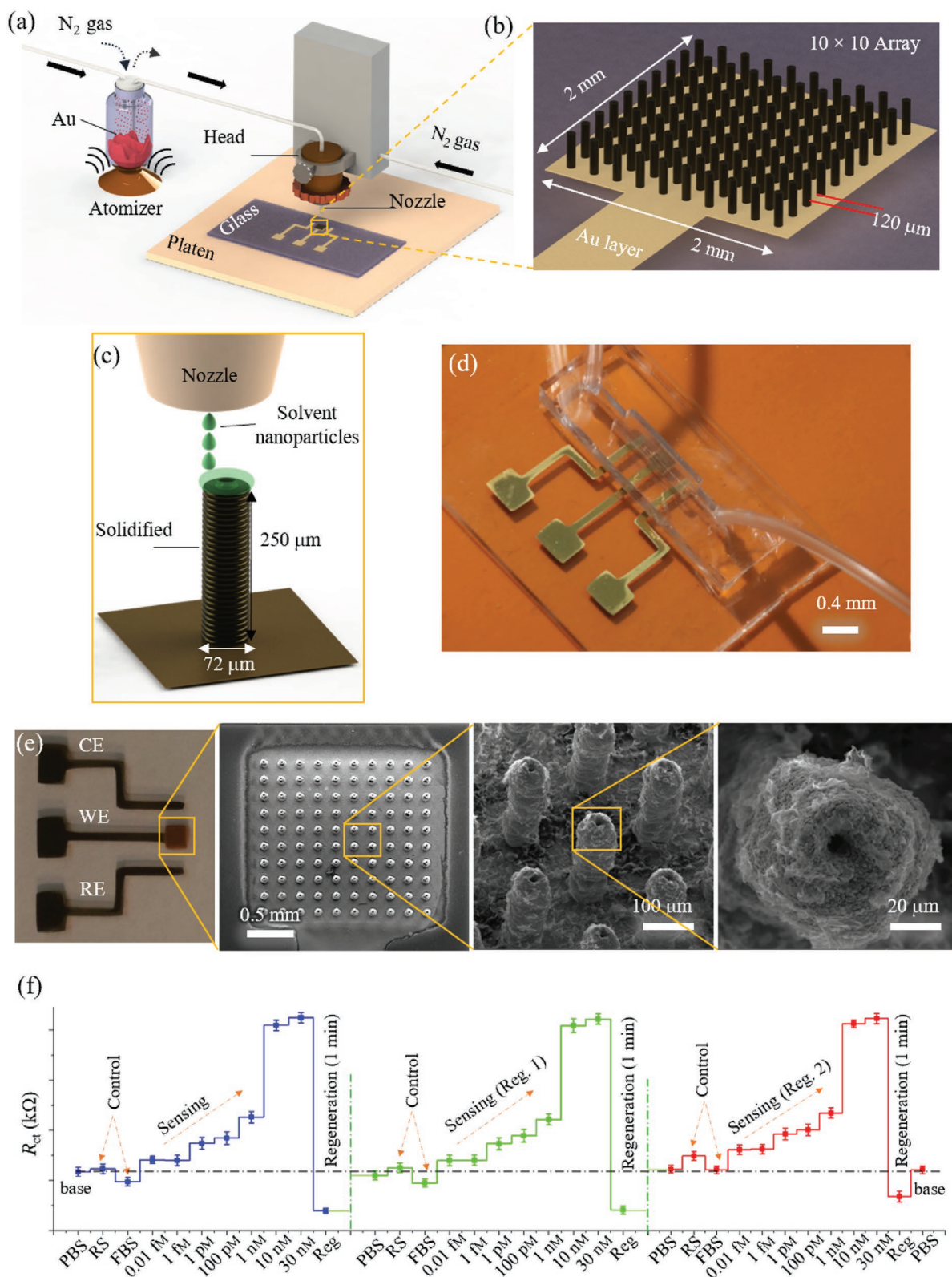


**Figure 6.** 3D printed biosensors for rapid and sensitive pathogen detection. a–c) Schematics showing AJP of biosensor for COVID-19 antibody detection in seconds.<sup>[33]</sup> The biosensor consisted of a 10 × 10 micropillar array coated with viral antigens as the working electrode. d, e) Optical image and SEM of the sensor depicted in (a), respectively. The SEM images show top view of the 3D printed micropillar array. f) Plots showing the sensing of spike S1 antibodies with repeated regeneration. The charge transfer resistance varies with the antibody concentration. For control studies, rabbit serum (RS) and fetal bovine serum (FBS) solution were used.<sup>[33]</sup> Reproduced with permission.<sup>[33]</sup> Copyright 2020, Wiley-VCH.

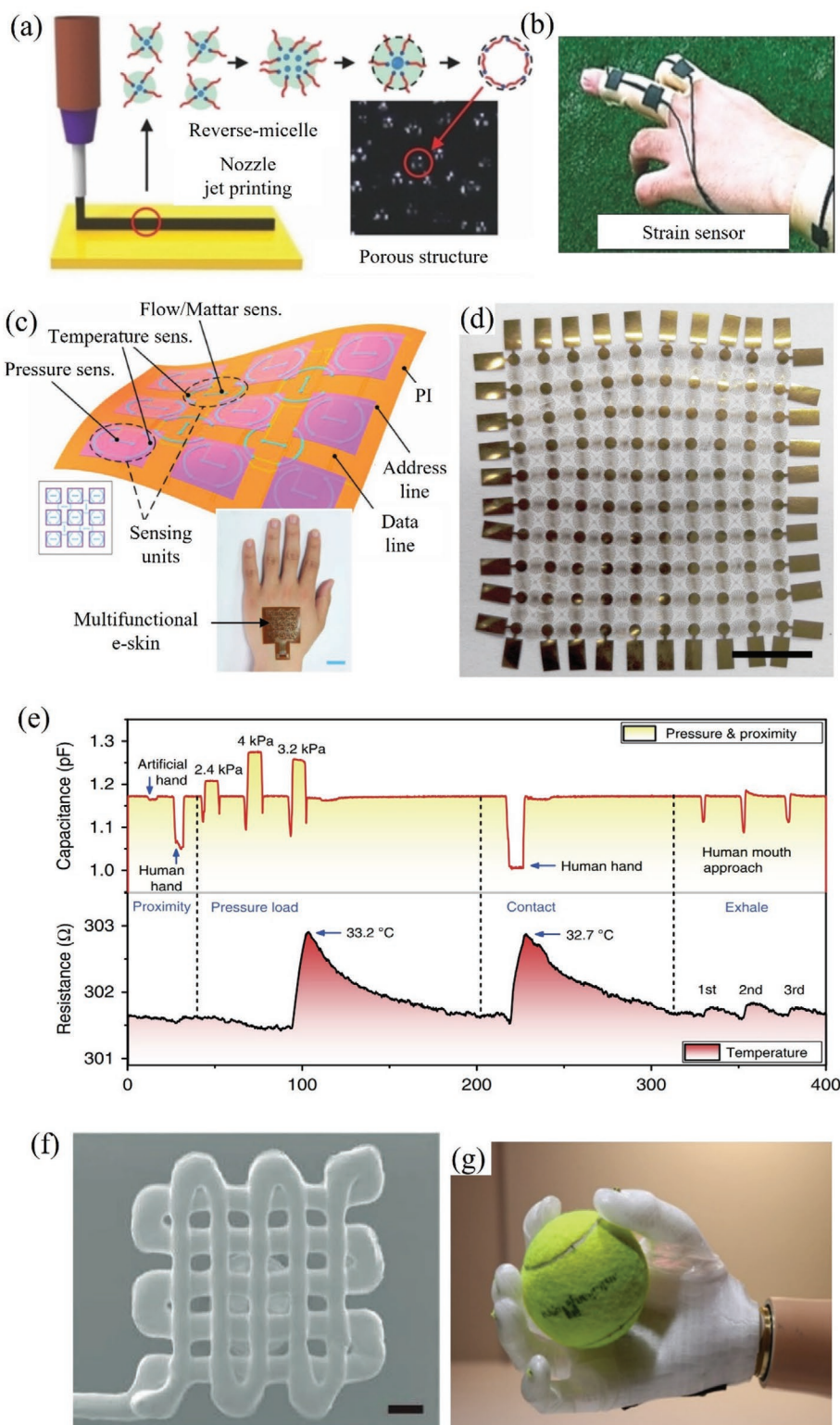


**Figure 7.** 3D printed physical sensors. a,b) Schematic demonstration of material jetting (extrusion printing) in combination with reverse micelle to create patterned PSR.<sup>[11]</sup> The use of such a sensor to monitor deformation/strain on a human finger is shown in (b). Reproduced with permission.<sup>[11]</sup> Copyright 2014, Wiley-VCH. c) A multifunctional electronic skin (e-skin) with multimodal sensing capability that demonstrates miniaturization and elasticity enabled by 3D printing.<sup>[183]</sup> Inset shows e-skin attached on the hand. Reproduced with permission.<sup>[183]</sup> Copyright 2017, Wiley-VCH. d) Another example of 3D printed electronic skin comprising of highly stretchable and conformable conductive matrix network on polyimide substrate for multifunctional sensing (10 × 10 sensor array, scale bar: 5 mm).<sup>[184]</sup> e) Real-time sensing of temperature, pressure, and proximity by the sensor shown in (d).<sup>[184]</sup> f) A tactile sensor with the SEM showing the printed device (scale bar is 200  $\mu\text{m}$ ).<sup>[5a]</sup> Reproduced with permission.<sup>[5a]</sup> Copyright 2017, Wiley-VCH. g) A prosthetic hand that uses 3D printed pressure sensors for controlling the grip. Handling of a spherical object was used to demonstrate the pressure control.<sup>[185]</sup>



to accelerate haptic perception. Further, a low-cost, kinesthetic haptic device named “Haptik” has been fabricated by Stanford University using 3D printing and used to educate middle school students.<sup>[189]</sup> Attempts have also been made to integrate augmented reality into haptic devices via 3D printing. A haptic device (Tooketo) was developed that integrated touch and audio sensing with the ability to receive audio information during its use.<sup>[190]</sup> In another example, a 3D multiaxial force sensor was developed using FDM<sup>[191]</sup> wherein the structural part was made of thermoplastic polyurethane and the sensing part was made of CNT-polymer nanocomposite. Such an arrangement of material provided a seamless integration of different components into the device. Apart from these, a miniature body-powered passive prosthetic hand was developed with a kinesthetic feedback by incorporating a force sensor and coin-type vibration motor.<sup>[192]</sup> In another recent work, a 3D printed prosthetic arm and a pressure sensing haptic system were integrated to enable the capture of objects such as a cricket ball (Figure 7g).<sup>[185]</sup> As the haptic sensors/interfaces evolve to include the IoT technologies, a deeper understanding and integration of biology, 3D printed electronics, and robotic systems are required for further developments in the field of physical biosensors.

## 7. Discussion and Future Directions

The miniaturization, personalization, and elasticity trends supported by 3D printing open novel avenues in biosensing that can provide long-term benefits to human health. Better still, these advances are only in their infancy, with several new AM methods on the horizon.<sup>[193]</sup> Thus, this review should be taken as an intermediate snapshot and a forward-thinking report.

The new developments in this field are highlighted by advances in the 3D printing technology itself, enabling new capabilities and functionalities in biosensors. These advances include multi-material printing, multi-length scale printing, and scale-up, which are being pursued by various labs and companies throughout the world. Recently, Aniwaa Pte. Ltd. has introduced a XJet 3D printer which has thousands of nozzles for the deposition of ceramics and metals to form 3D structures with part consolidation at 300 °C.<sup>[194]</sup> This technique offers a 5× increase in speed of manufacture by 3D printing. This technology has the potential of being used for the mass production of biosensors. Advanced 2PP printing was introduced recently by Nanoscribe GmbH to print polymeric structures at nanometer resolution which is not possible by other 3D printers.<sup>[195]</sup> For example, 3D conical nanostructures of carbon were realized by this method with two-steps thermal annealing and an integration with chip-scale CMOS devices that can have wireless transmission capability.<sup>[195]</sup> Exaddon GmbH has created a novel 3D printing system where several metallic materials can be printed as 3D structures at length scales of 500 nm to a few micrometers in minutes, making it possible to make multi-material devices with precisely controlled topography and texture.<sup>[196]</sup> Other equipment manufacturers (e.g., nScript Inc.) have been integrating methods such as pick and place of semiconductor chips with jetting-based AM. Similarly, 3D printers with additional multiple printheads/nozzles are being developed to scale-up production rates for various industries,

including biomedical sensors. These developments are also addressing the current limitations of 3D printing such as post-processing compatibility, layer misalignment, over-extrusion, and anisotropic mechanical strength.<sup>[197]</sup> In addition, active research is also ongoing in the materials’ area to address issues such as distortion after sintering for metal and polymers parts.<sup>[198]</sup> We expect these developments to lead to several types of “all-3D-printed-sensors” in the future where it is possible to manufacture parts in simple 1–2 steps, namely, printing, followed by curing/sintering. In fact, we note some progress on this front where fully 3D printed devices were realized for a subset of biomedical sensors for glucose and DNA sensing.<sup>[199]</sup>

The extent of the devastation caused by the COVID-19 pandemic<sup>[176]</sup> emphasized the need for fungible manufacturing infrastructure for test kits/sensors for their on-demand production. Such a system can quickly change the types of sensors manufactured to respond to specific healthcare emergencies. The immense flexibility offered by 3D printing in terms of changing the production programs at a click of a button can be of significant value to address this need. Further, to address the logistics of device transportation, on-site production of sensors can be of significant value to address regional health outbreaks/emergencies. This is especially applicable to underserved areas within the country and globally. Again, low-cost 3D printers can be deployed in remote regions to address these needs. 3D printing is expected to emerge as a broadly deployable indispensable tool in the fight against healthcare emergencies. Last, personalized medicine is expected to grow as an important field in the future.<sup>[200]</sup> This area will require making sensing devices tailored to individuals where the flexibility offered by 3D printing will be highly useful.

In summary, advances in biomedical sensor devices have accompanied the progress in fabrication technologies. 3D printing is an emerging manufacturing method that offers a) an ability to print a variety of geometries with a high level of complexity and customizability, b) rapid prototyping, c) waste minimization, and d) multi-material integration. These fabrication advantages have profoundly affected the biomedical sensors and fueled the trends of miniaturization/integration (for both Si-based devices and electronic packaging), ‘elasticity’ (i.e., devices with elastic modulus matching that of the biological tissue), and device personalization. In addition, 3D printing of biomedical sensors has the advantage that it can be done close to the place of consumption and does not need expensive clean-room facilities. This is especially advantageous when addressing the healthcare needs of populations in underserved areas. Across a range of sensors, 3D printing enables low LoD, high reproducibility, and a high degree of integration/complexity of the devices, with continued innovations for the foreseeable future.

## Acknowledgements

The authors gratefully acknowledge financial support from the NIH BRAIN Initiative R01 award number # RF1NS110483. The authors thank Prof. Tzahi Cohen-Karni at Carnegie Mellon University for valuable suggestions.

## Conflict of Interest

The authors declare no conflict of interest.

## Keywords

3D bio/chemical sensors, 3D printing, bioprinting, electrophysiological sensors, functional sensors, microfluidic structures, neural probes

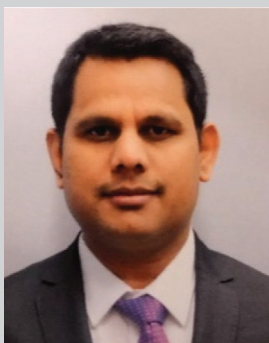
Received: August 4, 2021  
Revised: November 5, 2021  
Published online:

- [1] a) W. Greatbatch, United States patent #3478746, **1969**;  
b) W. Greatbatch, United States patent 3057356, **1962**.
- [2] J. Kim, A. S. Campbell, B. E.-F. de Ávila, J. Wang, *Nat. Biotechnol.* **2019**, *37*, 389.
- [3] a) J. Shi, Y. Fang, *Adv. Mater.* **2019**, *31*, 1804895; b) C. Lu, U. P. Froriep, R. A. Koppes, A. Canales, V. Caggiano, J. Selvidge, E. Bizzi, P. Anikeeva, *Adv. Funct. Mater.* **2014**, *24*, 6594.
- [4] C. Zhou, W. Xu, P. Zhang, M. Jiang, Y. Chen, R. T. Kwok, M. M. Lee, G. Shan, R. Qi, X. Zhou, *Adv. Funct. Mater.* **2019**, *29*, 1805986.
- [5] a) S.-Z. Guo, K. Qiu, F. Meng, S. H. Park, M. C. McAlpine, *Adv. Mater.* **2017**, *29*, 1701218; b) Y. Wan, Y. Wang, C. F. Guo, *Mater. Today Phys.* **2017**, *1*, 61.
- [6] a) M. A. Ali, S. Tabassum, Q. Wang, Y. Wang, R. Kumar, L. Dong, *Lab Chip* **2018**, *18*, 803; b) P. Saccomandi, E. Schena, C. M. Oddo, L. Zollo, S. Silvestri, E. Guglielmelli, *Biosensors* **2014**, *4*, 422.
- [7] M.-Y. Li, S.-K. Su, H.-S. P. Wong, L.-J. Li, *Nature* **2019**, *567*, 169.
- [8] R. Mahajan, Z. Qian, R. S. Viswanath, S. Srinivasan, K. Aygün, W.-L. Jen, S. Sharan, A. Dhall, *IEEE Trans. Compon., Packag., Manuf. Technol.* **2019**, *9*, 1952.
- [9] R. Muller, H.-P. Le, W. Li, P. Ledochowitsch, S. Gambini, T. Bjorninen, A. Koralek, J. M. Carmena, M. M. Maharbiz, E. Alon, presented at 2014 IEEE Int. Solid-State Circuits Conf. Digest of Technical Papers (ISSCC), IEEE, San Francisco, CA **2014**.
- [10] H.-J. Chung, M. S. Sulkin, J.-S. Kim, C. Goudeseune, H.-Y. Chao, J. W. Song, S. Y. Yang, Y.-Y. Hsu, R. Ghaffari, I. R. Efimov, *Adv. Healthcare Mater.* **2014**, *3*, 59.
- [11] S. Jung, J. H. Kim, J. Kim, S. Choi, J. Lee, I. Park, T. Hyeon, D.-H. Kim, *Adv. Mater.* **2014**, *26*, 4825.
- [12] M. E. Rouse, A. Azocar, L. Hargrove, *Nat. Biomed. Eng.* **2020**, *4*, 933.
- [13] J. Zhou, D. A. Khodakov, A. V. Ellis, N. H. Voelcker, *Electrophoresis* **2012**, *33*, 89.
- [14] a) M. L. Griffith, *Doctoral Thesis*, University of Michigan **1995**;  
b) J. Ni, H. Ling, S. Zhang, Z. Wang, Z. Peng, C. Benyshek, R. Zan, A. Miri, Z. Li, X. Zhang, *Mater. Today Bio* **2019**, *3*, 100024.
- [15] X. Zhang, X. Jiang, C. Sun, *Sens. Actuators, A* **1999**, *77*, 149.
- [16] a) A. P. Kuo, N. Bhattacharjee, Y. S. Lee, K. Castro, Y. T. Kim, A. Folch, *Adv. Mater. Technol.* **2019**, *4*, 1800395; b) K. Piironen, M. Haapala, V. Talman, P. Järvinen, T. Sikanen, *Lab Chip* **2020**, *20*, 2372.
- [17] S. Takenaga, B. Schneider, E. Erbay, M. Biselli, T. Schnitzler, M. J. Schöning, T. Wagner, *Phys. Status Solidi A* **2015**, *212*, 1347.
- [18] K. Ikuta, K. Hirowatari, T. Ogata, presented at Proc. IEEE micro electro mechanical systems an investigation of micro structures, sensors, actuators, machines and robotic systems, IEEE, Oiso, Japan **1994**.
- [19] K. Kadimisetty, S. Malla, J. F. Rusling, *ACS Sens.* **2017**, *2*, 670.
- [20] A. Frutiger, J. T. Muth, D. M. Vogt, Y. Mengüç, A. Campo, A. D. Valentine, C. J. Walsh, J. A. Lewis, *Adv. Mater.* **2015**, *27*, 2440.
- [21] S. Harada, K. Kanao, Y. Yamamoto, T. Arie, S. Akita, K. Takei, *ACS Nano* **2014**, *8*, 12851.
- [22] P. Alto, *Met. Powder Rep.* **2014**, *69*, 42.
- [23] J.-W. Choi, E. MacDonald, R. Wicker, *Int. J. Adv. Manuf. Technol.* **2010**, *49*, 543.
- [24] A. Standard, *Standard terminology for additive manufacturing technologies*, ASTM International, West Conshohocken **2012**.
- [25] D. Qin, Y. Xia, G. M. Whitesides, *Nat. Protoc.* **2010**, *5*, 491.
- [26] E. Lindner, R. P. Buck, *Anal. Chem.* **2000**, *72*, 336 A.
- [27] C. W. Hull, United States patent 5236637, **1993**.
- [28] J. Manriquez-Frayre, D. Bourell, presented in Solid Freeform Fabrication Symp, Austin, TX **1990**.
- [29] F. Oberpenning, J. Meng, J. J. Yoo, A. Atala, *Nat. Biotechnol.* **1999**, *17*, 149.
- [30] W. Wu, A. DeConinck, J. A. Lewis, *Adv. Mater.* **2011**, *23*, H178.
- [31] S. A. Gowers, V. F. Curto, C. A. Seneci, C. Wang, S. Anastasova, P. Vadgama, G.-Z. Yang, M. G. Boutelle, *Anal. Chem.* **2015**, *87*, 7763.
- [32] G. Papadakis, A. K. Pantazis, M. Ntogka, K. Parasyris, G.-I. Theodosi, G. Kaprou, E. Gizeli, *ACS Sens.* **2019**, *4*, 1329.
- [33] M. A. Ali, C. Hu, S. Jahan, B. Yuan, M. S. Saleh, E. Ju, S.-J. Gao, R. P. Panat, *Adv. Mater.* **2020**, *33*, 2006647.
- [34] T. Kim, Q. Yi, E. Hoang, R. Esfandyarpour, *Adv. Mater. Technol.* **2021**, *6*, 2001021.
- [35] A. M. Paterson, E. Donnison, R. J. Bibb, R. I. Campbell, *Hand Ther.* **2014**, *19*, 102.
- [36] V. Khare, S. Sonkaria, G.-Y. Lee, S.-H. Ahn, W.-S. Chu, *Int. J. Precis. Eng. Manuf.-Green Technol.* **2017**, *4*, 291.
- [37] L. Clark Jr., C. Lyons, *Ann. N. Y. Acad. Sci.* **1962**, *102*, 29.
- [38] J. L. Erkal, A. Selimovic, B. C. Gross, S. Y. Lockwood, E. L. Walton, S. McNamara, R. S. Martin, D. M. Spence, *Lab Chip* **2014**, *14*, 2023.
- [39] M. S. Saleh, S. Ritchie, M. A. Nicholas, R. Bezbaruah, J. W. Reddy, M. Chamanzar, E. A. Yttri, R. Panat, *bioRxiv* **2019**, 742346.
- [40] A. H. Gittis, E. A. Yttri, *Curr. Opin. Biomed. Eng.* **2018**, *8*, 14.
- [41] A. I. Shalhan, P. Smejkal, M. Corban, R. M. Guitj, M. C. Breadmore, *Anal. Chem.* **2014**, *86*, 3124.
- [42] J. U. Lind, T. A. Busbee, A. D. Valentine, F. S. Pasqualini, H. Yuan, M. Yadid, S.-J. Park, A. Kotikian, A. P. Nesmith, P. H. Campbell, *Nat. Mater.* **2017**, *16*, 303.
- [43] H.-G. Yi, Y. H. Jeong, Y. Kim, Y.-J. Choi, H. E. Moon, S. H. Park, K. S. Kang, M. Bae, J. Jang, H. Youn, *Nat. Biomed. Eng.* **2019**, *3*, 509.
- [44] H. Ota, M. Chao, Y. Gao, E. Wu, L.-C. Tai, K. Chen, Y. Matsuoka, K. Iwai, H. M. Fahad, W. Gao, *ACS Sens.* **2017**, *2*, 990.
- [45] K. Kim, J. Choi, Y. Jeong, I. Cho, M. Kim, S. Kim, Y. Oh, I. Park, *Adv. Healthcare Mater.* **2019**, *8*, 1900978.
- [46] A. Bandyopadhyay, B. Heer, *Mater. Sci. Eng., R* **2018**, *129*, 1.
- [47] P. E. Sheehan, L. J. Whitman, *Nano Lett.* **2005**, *5*, 803.
- [48] L. Soleymani, Z. Fang, E. H. Sargent, S. O. Kelley, *Nat. Nanotechnol.* **2009**, *4*, 844.
- [49] M. A. Ali, C. Hu, B. Yuan, S. Jahan, M. S. Saleh, Z. Guo, A. Gellman, R. Panat, *Nat. Comm* **2021**.
- [50] J. H. Jang, C. K. Ullal, M. Maldovan, T. Gorishnyy, S. Kooi, C. Koh, E. L. Thomas, *Adv. Funct. Mater.* **2007**, *17*, 3027.
- [51] W. Chu, Y. Tan, P. Wang, J. Xu, W. Li, J. Qi, Y. Cheng, *Adv. Mater. Technol.* **2018**, *3*, 1700396.
- [52] M. S. Saleh, C. Hu, R. Panat, *Sci. Adv.* **2017**, *3*, e1601986.
- [53] a) R. Rebelo, A. I. Barbosa, D. Caballero, I. K. Kwon, J. M. Oliveira, S. C. Kundu, R. L. Reis, V. M. Correlo, *Biosens. Bioelectron.* **2019**, *130*, 20; b) A. I. Barbosa, N. M. Reis, *Analyst* **2017**, *142*, 858; c) T. Bertok, A. Sediva, A. Vikartovska, J. Tkac, *Int. J. Electrochem. Sci.* **2014**, *9*, 890.
- [54] H. Yang, M. T. Rahman, D. Du, R. Panat, Y. Lin, *Sens. Actuators, B* **2016**, *230*, 600.
- [55] I. C. Samper, S. A. Gowers, M. L. Rogers, D.-S. R. Murray, S. L. Jewell, C. Pahl, A. J. Strong, M. G. Boutelle, *Lab Chip* **2019**, *19*, 2038.
- [56] A. H. Loo, C. K. Chua, M. Pumera, *Analyst* **2017**, *142*, 279.
- [57] S. S. Hinman, K. S. McKeating, Q. Cheng, *Anal. Chem.* **2017**, *89*, 12626.

- [58] A. I. Aristov, M. Manousidaki, A. Danilov, K. Terzaki, C. Fotakis, M. Farsari, A. V. Kabashin, *Sci. Rep.* **2016**, *6*, 25380.
- [59] C. Ma, Y. Peng, H. Li, W. Chen, *Trends Pharmacol. Sci.* **2020**, *42*, 119.
- [60] M. T. Rahman, A. Rahimi, S. Gupta, R. Panat, *Sens. Actuators, A* **2016**, *248*, 94.
- [61] S. Baik, N. Kim, T.-i. Kim, H. Chae, K. H. Kim, C. Pang, K.-Y. Suh, *Curr. Appl. Phys.* **2015**, *15*, 274.
- [62] M. Nikzad, S. H. Masood, I. Sbarski, *Mater. Des.* **2011**, *32*, 3448.
- [63] G. Gaal, M. Mendes, T. P. de Almeida, M. H. O. Piazzetta, Á. L. Gobbi, A. Riul, V. Rodrigues, *Sens. Actuators, B* **2017**, *242*, 35.
- [64] E. Masaeli, C. Marquette, *Front. Bioeng. Biotechnol.* **2020**, *7*, 478.
- [65] B. Kim, A. H. Soepriatna, W. Park, H. Moon, A. Cox, J. Zhao, N. S. Gupta, C. H. Park, K. Kim, Y. Jeon, *Nat. Commun.* **2021**, *12*, 3710.
- [66] C. J. Hansen, R. Saksena, D. B. Kolesky, J. J. Vericella, S. J. Kranz, G. P. Muldowney, K. T. Christensen, J. A. Lewis, *Adv. Mater.* **2013**, *25*, 96.
- [67] R. L. Truby, J. A. Lewis, *Nature* **2016**, *540*, 371.
- [68] Y. J. Lee, P. V. Braun, *Adv. Mater.* **2003**, *15*, 563.
- [69] D. Theriault, S. R. White, J. A. Lewis, *Nat. Mater.* **2003**, *2*, 265.
- [70] L. G. Griffith, G. Naughton, *Science* **2002**, *295*, 1009.
- [71] M. A. Skylar-Scott, S. Gunasekaran, J. A. Lewis, *Proc. Natl. Acad. Sci. U. S. A.* **2016**, *113*, 6137.
- [72] Y. Y. Li, F. Cunin, J. R. Link, T. Gao, R. E. Betts, S. H. Reiver, V. Chin, S. N. Bhatia, M. J. Sailor, *Science* **2003**, *299*, 2045.
- [73] S. D. Gittard, A. Nguyen, K. Obata, A. Koroleva, R. J. Narayan, B. N. Chichkov, *Biomed. Opt. Express* **2011**, *2*, 3167.
- [74] J. A. Kim, D. J. Wales, A. J. Thompson, G. Z. Yang, *Adv. Opt. Mater.* **2020**, *8*, 1901934.
- [75] C. Ude, T. Hentrop, P. Lindner, T. H. Lücking, T. Scheper, S. Beutel, *Sens. Actuators, B* **2015**, *221*, 1035.
- [76] K. Fukuda, T. Minamiki, T. Minami, M. Watanabe, T. Fukuda, D. Kumaki, S. Tokito, *Adv. Electron. Mater.* **2015**, *1*, 1400052.
- [77] L. Faller, W. Granig, M. Krivec, A. Abram, H. Zangl, *J. Micromech. Microeng.* **2018**, *28*, 104002.
- [78] a) A. Pugalendhi, R. Ranganathan, S. Ganesan, *Mater. Today: Proc.* **2021**, *46*, 9139; b) G. Kim, Y. Oh, *Proc. Inst. Mech. Eng., Part B* **2008**, *222*, 201; c) P. Gay, D. Blanco, F. Pelayo, A. Noriega, P. Fernández, *Proc. Eng.* **2015**, *132*, 70.
- [79] C. Didier, A. Kundu, S. Rajaraman, *Microsyst. Nanoeng.* **2020**, *6*, 15.
- [80] J. Brennehan, D. Tansel, G. Fedder, R. Panat, *Extreme Mech. Lett.* **2021**, *43*, 101199.
- [81] Q. Jing, Y. S. Choi, M. Smith, C. Ou, T. Busolo, S. Kar-Narayan, *Adv. Mater. Technol.* **2019**, *4*, 1900048.
- [82] I. Gibson, D. Rosen, B. Stucker, M. Khorasani, in *Additive Manufacturing Technologies*, Springer, Cham, Switzerland **2021**, p. 203.
- [83] a) M. Sadeq Saleh, M. HamidVishkasouh, H. Zbib, R. Panat, *Scr. Mater.* **2018**, *149*, 144; b) M. S. Saleh, C. Hu, J. Brennehan, A. M. Al Mutairi, R. Panat, *Addit. Manuf.* **2021**, *39*, 101856.
- [84] K. Li, H. Wei, W. Liu, H. Meng, P. Zhang, C. Yan, *Nanotechnology* **2018**, *29*, 185501.
- [85] a) L. Grob, P. Rinklin, S. Zips, D. Mayer, S. Weidlich, K. Terkan, L. J. Weiß, N. Adly, A. Offenhäusser, B. Wolfrum, *Sensors* **2021**, *21*, 3981; b) L. Grob, H. Yamamoto, S. Zips, P. Rinklin, A. Hirano-Iwata, B. Wolfrum, *Adv. Mater. Technol.* **2020**, *5*, 1900517.
- [86] M. D. Dankoco, G. Y. Tesfay, E. Benevent, M. Bendahan, *Mater. Sci. Eng., B* **2016**, *205*, 1.
- [87] N. G. Di Novo, E. Cantù, S. Tonello, E. Sardini, M. Serpelloni, *Sensors* **2019**, *19*, 1842.
- [88] T. Rahman, L. Renaud, D. Heo, M. Renn, R. Panat, *J. Micromech. Microeng.* **2015**, *25*, 107002.
- [89] L. Gagné, G. Rivera, G. Laroche, *Biomaterials* **2006**, *27*, 5430.
- [90] S. Agarwala, G. L. Goh, T.-S. D. Le, J. An, Z. K. Peh, W. Y. Yeong, Y.-J. Kim, *ACS Sens.* **2019**, *4*, 218.
- [91] B. J. Rumley-Ouellette, J. H. Wahry, A. M. Baker, J. D. Bernardin, A. N. Marchi, M. D. Todd, *Struct. Health Monit.* **2017**, 1881.
- [92] S. Bose, A. Bandyopadhyay, in *Additive manufacturing*, CRC Press, Boca Raton **2019**, p. 451.
- [93] T. N. A. T. Rahim, A. M. Abdullah, H. M. Akil, *Polym. Rev.* **2019**, *59*, 589.
- [94] H. Ravanbakhsh, G. Bao, Z. Luo, L. G. Mongeau, Y. S. Zhang, *ACS Biomater. Sci. Eng.* **2021**, *7*, 4009.
- [95] S. Chen, M. Su, C. Zhang, M. Gao, B. Bao, Q. Yang, B. Su, Y. Song, *Adv. Mater.* **2015**, *27*, 3928.
- [96] J. Z. Manapat, Q. Chen, P. Ye, R. C. Advincula, *Macromol. Mater. Eng.* **2017**, *302*, 1600553.
- [97] Z. Wang, H. Kumar, Z. Tian, X. Jin, J. F. Holzman, F. Menard, K. Kim, *ACS Appl. Mater. Interfaces* **2018**, *10*, 26859.
- [98] T. M. Valentin, S. E. Leggett, P.-Y. Chen, J. K. Sodhi, L. H. Stephens, H. D. McClintock, J. Y. Sim, I. Y. Wong, *Lab Chip* **2017**, *17*, 3474.
- [99] K.-W. Lee, S. Wang, B. C. Fox, E. L. Ritman, M. J. Yaszemski, L. Lu, *Biomacromolecules* **2007**, *8*, 1077.
- [100] F. P. Melchels, J. Feijen, D. W. Grijpma, *Biomaterials* **2010**, *31*, 6121.
- [101] K. M. Arif, T. Murakami, *Int. J. Adv. Manuf. Technol.* **2009**, *41*, 527.
- [102] M. Sharafeldin, A. Jones, J. F. Rusling, *Micromachines* **2018**, *9*, 394.
- [103] L. Ge, L. Dong, D. Wang, Q. Ge, G. Gu, *Sens. Actuators, A* **2018**, *273*, 285.
- [104] R. B. Osman, A. J. van der Veen, D. Huiberts, D. Wismeijer, N. Alharbi, *J. Mech. Behav. Biomed. Mater.* **2017**, *75*, 521.
- [105] O. Santoliquido, P. Colombo, A. Ortona, *J. Eur. Ceram. Soc.* **2019**, *39*, 2140.
- [106] Z. Huang, G. C.-P. Tsui, Y. Deng, C.-Y. Tang, *Nanotechnol. Rev.* **2020**, *9*, 1118.
- [107] T. M. Hsieh, C. W. B. Ng, K. Narayanan, A. C. Wan, J. Y. Ying, *Biomaterials* **2010**, *31*, 7648.
- [108] M. A. Haque, N. V. Lavrik, D. Hensley, N. McFarlane, presented at *2019 IEEE 69th Electronic Components and Technology Conf. (ECTC)*, IEEE, Las Vegas, NV, USA **2019**.
- [109] M. Farsari, B. N. Chichkov, *Nat. Photonics* **2009**, *3*, 450.
- [110] K. H. Tan, C. K. Chua, K. F. Leong, C. M. Cheah, P. Cheang, M. S. Abu Bakar, S. W. Cha, *Biomaterials* **2003**, *24*, 3115.
- [111] A. Awad, F. Fina, A. Goyanes, S. Gaisford, A. W. Basit, *Int. J. Pharm.* **2020**, *586*, 119594.
- [112] K. Dotchev, W. Yusoff, *Rapid Prototyping J.* **2009**, *15*, 192.
- [113] R. P. Tortorich, J.-W. Choi, *Nanomaterials* **2013**, *3*, 453.
- [114] M. S. Mannoor, Z. Jiang, T. James, Y. L. Kong, K. A. Malatesta, W. O. Soboyejo, N. Verma, D. H. Gracias, M. C. McAlpine, *Nano Lett.* **2013**, *13*, 2634.
- [115] Z.-X. Low, Y. T. Chua, B. M. Ray, D. Mattia, I. S. Metcalfe, D. A. Patterson, *J. Membr. Sci.* **2017**, *523*, 596.
- [116] E. A. Roth, T. Xu, M. Das, C. Gregory, J. J. Hickman, T. Boland, *Biomaterials* **2004**, *25*, 3707.
- [117] J. Kastner, T. Faury, H. M. Außerhuber, T. Obermüller, H. Leichtfried, M. J. Haslinger, E. Liftinger, J. Innerlohinger, I. Gnatiuk, D. Holzinger, *Microelectron. Eng.* **2017**, *176*, 84.
- [118] A. Hudd, *The chemistry of inkjet inks*, World Scientific **2011**, 3.
- [119] G. L. Goh, S. Agarwala, W. Y. Yeong, *ACS Appl. Mater. Interfaces* **2019**, *11*, 43719.
- [120] I. Grunwald, E. Groth, I. Wirth, J. Schumacher, M. Maiwald, V. Zoellmer, M. Busse, *Biofabrication* **2010**, *2*, 014106.
- [121] A. A. Gupta, A. Bolduc, S. G. Cloutier, R. Izquierdo, presented at *2016 IEEE Int. Symp. on Circuits and Systems (ISCAS)*, IEEE, Montreal, QC, Canada **2016**.
- [122] M. S. Saleh, J. Li, J. Park, R. Panat, *Addit. Manuf.* **2018**, *23*, 70.
- [123] G. M. Whitesides, *Nature* **2006**, *442*, 368.
- [124] H. N. Chan, Y. Shu, B. Xiong, Y. Chen, Y. Chen, Q. Tian, S. A. Michael, B. Shen, H. Wu, *ACS Sens.* **2016**, *1*, 227.

- [125] A. K. Au, N. Bhattacharjee, L. F. Horowitz, T. C. Chang, A. Folch, *Lab Chip* **2015**, *15*, 1934.
- [126] T. N. Nguyen, J. K. Nolan, H. Park, S. Lam, M. Fattah, J. C. Page, H.-E. Joe, M. B. Jun, H. Lee, S. J. Kim, *Biosens. Bioelectron.* **2019**, *131*, 257.
- [127] B. N. Johnson, K. Z. Lancaster, I. B. Hogue, F. Meng, Y. L. Kong, L. W. Enquist, M. C. McAlpine, *Lab Chip* **2016**, *16*, 1393.
- [128] C. L. Sones, S. Mailis, W. S. Brocklesby, R. W. Eason, J. R. Owen, *J. Mater. Chem.* **2002**, *12*, 295.
- [129] E. Cesewski, A. P. Haring, Y. Tong, M. Singh, R. Thakur, S. Laheri, K. A. Read, M. D. Powell, K. J. Oestreich, B. N. Johnson, *Lab Chip* **2018**, *18*, 2087.
- [130] A. Kamyshny, S. Magdassi, *Chem. Soc. Rev.* **2019**, *48*, 1712.
- [131] T. N. H. Nguyen, J. K. Nolan, H. Park, S. Lam, M. Fattah, J. C. Page, H.-E. Joe, M. B. G. Jun, H. Lee, S. J. Kim, R. Shi, H. Lee, *Biosens. Bioelectron.* **2019**, *131*, 257.
- [132] R. Herbert, S. Mishra, H. R. Lim, H. Yoo, W. H. Yeo, *Adv. Sci.* **2019**, *6*, 1970110.
- [133] Z. Pu, J. Tu, R. Han, X. Zhang, J. Wu, C. Fang, H. Wu, X. Zhang, H. Yu, D. Li, *Lab Chip* **2018**, *18*, 3570.
- [134] D. Huh, G. A. Hamilton, D. E. Ingber, *Trends Cell Biol.* **2011**, *21*, 745.
- [135] A. Bouchie, L. DeFrancesco, *Nat. Biotechnol.* **2015**, *33*, 247.
- [136] K. H. Benam, R. Villenave, C. Lucchesi, A. Varone, C. Hubeau, H.-H. Lee, S. E. Alves, M. Salmon, T. C. Ferrante, J. C. Weaver, A. Bahinski, G. A. Hamilton, D. E. Ingber, *Nat. Methods* **2016**, *13*, 151.
- [137] J. W. Lee, Y.-J. Choi, W.-J. Yong, F. Pati, J.-H. Shim, K. S. Kang, I.-H. Kang, J. Park, D.-W. Cho, *Biofabrication* **2016**, *8*, 015007.
- [138] L. Horváth, Y. Umehara, C. Jud, F. Blank, A. Petri-Fink, B. Rothen-Rutishauser, *Sci. Rep.* **2015**, *5*, 7974.
- [139] K. A. Homan, N. Gupta, K. T. Kroll, D. B. Kolesky, M. Skylar-Scott, T. Miyoshi, D. Mau, M. T. Valerius, T. Ferrante, J. V. Bonventre, J. A. Lewis, R. Morizane, *Nat. Methods* **2019**, *16*, 255.
- [140] A. Skardal, S. V. Murphy, M. Devarasetty, I. Mead, H.-W. Kang, Y.-J. Seol, Y. Shrike Zhang, S.-R. Shin, L. Zhao, J. Aleman, A. R. Hall, T. D. Shupe, A. Kleensang, M. R. Dokmeci, S. Jin Lee, J. D. Jackson, J. J. Yoo, T. Hartung, A. Khademhosseini, S. Soker, C. E. Bishop, A. Atala, *Sci. Rep.* **2017**, *7*, 8837.
- [141] Y. S. Zhang, A. Arneri, S. Bersini, S.-R. Shin, K. Zhu, Z. Goli-Malekbadai, J. Aleman, C. Colosi, F. Busignani, V. Dell'Erbia, C. Bishop, T. Shupe, D. Demarchi, M. Moretti, M. Rasponi, M. R. Dokmeci, A. Atala, A. Khademhosseini, *Biomaterials* **2016**, *110*, 45.
- [142] Y. Wang, L. Wang, Y. Guo, Y. Zhu, J. Qin, *RSC Adv.* **2018**, *8*, 1677.
- [143] K. K. Lee, H. A. McCauley, T. R. Broda, M. J. Kofron, J. M. Wells, C. I. Hong, *Lab Chip* **2018**, *18*, 3079.
- [144] K. Kadimisetty, I. M. Mosa, S. Malla, J. E. Satterwhite-Warden, T. M. Kuhns, R. C. Faria, N. H. Lee, J. F. Rusling, *Biosens. Bioelectron.* **2016**, *77*, 188.
- [145] D. Chudobova, K. Cihalova, S. Skalickova, J. Zitka, M. A. M. Rodrigo, V. Milosavljevic, D. Hynek, P. Kopel, R. Vesely, V. Adam, *Electrophoresis* **2015**, *36*, 457.
- [146] W. Lee, D. Kwon, W. Choi, G. Y. Jung, A. K. Au, A. Folch, S. Jeon, *Sci. Rep.* **2015**, *5*, 18833.
- [147] W. Ling, G. Liew, Y. Li, Y. Hao, H. Pan, H. Wang, B. Ning, H. Xu, X. Huang, *Adv. Mater.* **2018**, *30*, 1800917.
- [148] C. Yang, Q. Cao, P. Puthongkham, S. T. Lee, M. Ganesana, N. V. Lavrik, B. J. Venton, *Angew. Chem., Int. Ed.* **2018**, *57*, 14255.
- [149] D. W. Kimmel, G. LeBlanc, M. E. Meschievitz, D. E. Cliffel, *Anal. Chem.* **2012**, *84*, 685.
- [150] a) C. Tang, A. Vaze, J. Rusling, *Lab Chip* **2017**, *17*, 484; b) D. A. Healy, C. J. Hayes, P. Leonard, L. McKenna, R. O'Kennedy, *Trends Biotechnol.* **2007**, *25*, 125.
- [151] Y. Zhao, S.-H. Li, J. Chu, Y.-P. Chen, W.-W. Li, H.-Q. Yu, G. Liu, Y.-C. Tian, Y. Xiong, *Biosens. Bioelectron.* **2012**, *35*, 115.
- [152] J. Zheng, X. Zhou, *Bioelectrochemistry* **2007**, *70*, 408.
- [153] S. Chung, M. H. Akhtar, A. Benboudiaf, D. S. Park, Y. B. Shim, *Electroanalysis* **2020**, *32*, 520.
- [154] C. Cao, J. P. Kim, B. W. Kim, H. Chae, H. C. Yoon, S. S. Yang, S. J. Sim, *Biosens. Bioelectron.* **2006**, *21*, 2106.
- [155] J. Yao, Y. Wang, Y. Dai, C. C. Liu, *ACS Omega* **2018**, *3*, 6411.
- [156] A. Manbohi, S. H. Ahmadi, *Sens. Bio-Sens. Res.* **2019**, *23*, 100270.
- [157] S. Nesaee, Y. Song, Y. Wang, X. Ruan, D. Du, A. Gozen, Y. Lin, *Anal. Chim. Acta* **2018**, *1043*, 142.
- [158] E. Bihar, S. Wustoni, A. M. Pappa, K. N. Salama, D. Baran, S. Inal, *npj Flexible Electron.* **2018**, *2*, 30.
- [159] J. Chen, W.-D. Zhang, J.-S. Ye, *Electrochem. Commun.* **2008**, *10*, 1268.
- [160] S. Y. Oh, S. Y. Hong, Y. R. Jeong, J. Yun, H. Park, S. W. Jin, G. Lee, J. H. Oh, H. Lee, S.-S. Lee, *ACS Appl. Mater. Interfaces* **2018**, *10*, 13729.
- [161] R. Pemberton, J. Xu, R. Pittson, N. Biddle, G. Drago, S. Jackson, J. Hart, *Anal. Biochem.* **2009**, *385*, 334.
- [162] E. H. Z. Ho, A. Ambrosi, M. Pumera, *Appl. Mater. Today* **2018**, *12*, 43.
- [163] X. Li, Y. Wang, J. Liu, M. Sun, X. Bo, H.-L. Wang, M. Zhou, *Electrochem. Commun.* **2017**, *82*, 139.
- [164] N. Puri, V. Sharma, V. K. Tanwar, N. Singh, A. M. Biradar, *Prog. Biomater.* **2013**, *2*, 5.
- [165] S. Shukla, X. Vidal, E. P. Furlani, M. T. Swihart, K.-T. Kim, Y.-K. Yoon, A. Urbas, P. N. Prasad, *ACS Nano* **2011**, *5*, 1947.
- [166] S. Shukla, E. P. Furlani, X. Vidal, M. T. Swihart, P. N. Prasad, *Adv. Mater.* **2010**, *22*, 3695.
- [167] Y. Liu, Q. Hu, F. Zhang, C. Tuck, D. Irvine, R. Hague, Y. He, M. Simonelli, G. A. Rance, E. F. Smith, *Polymers* **2016**, *8*, 325.
- [168] Q. Hu, X.-Z. Sun, C. D. Parmenter, M. W. Fay, E. F. Smith, G. A. Rance, Y. He, F. Zhang, Y. Liu, D. Irvine, *Sci. Rep.* **2017**, *7*, 17150.
- [169] H. Guner, E. Ozgur, G. Kokturk, M. Celik, E. Esen, A. E. Topal, S. Ayas, Y. Uludag, C. Elbuken, A. Dana, *Sens. Actuators, B* **2017**, *239*, 571.
- [170] Y. Chen, Q. Fu, D. Li, J. Xie, D. Ke, Q. Song, Y. Tang, H. Wang, *Anal. Bioanal. Chem.* **2017**, *409*, 6567.
- [171] A. K. Yetisen, M. S. Akram, C. R. Lowe, *Lab Chip* **2013**, *13*, 2210.
- [172] A. Youssef, S. J. Hollister, P. D. Dalton, *Biofabrication* **2017**, *9*, 012002.
- [173] D. Han, R. S. Morde, S. Mariani, A. A. La Mattina, E. Vignali, C. Yang, G. Barillaro, H. Lee, *Adv. Funct. Mater.* **2020**, *30*, 1909197.
- [174] D. Wasserberg, X. Zhang, C. Breukers, B. J. Connell, E. Baeten, D. van den Blink, È. S. Benet, A. C. Bloem, M. Nijhuis, A. M. J. Wensing, L. W. M. M. Terstappen, M. Beck, *Biosens. Bioelectron.* **2018**, *117*, 659.
- [175] Y. L. Kong, X. Zou, C. A. McCandler, A. R. Kirtane, S. Ning, J. Zhou, A. Abid, M. Jafari, J. Rogner, D. Minahan, *Adv. Mater. Technol.* **2019**, *4*, 1800490.
- [176] Johns Hopkins University Coronavirus Resource Website, <https://coronavirus.jhu.edu/map.html> (accessed: November 2021).
- [177] H. Shafee, M. Jahangir, F. Inci, S. Wang, R. B. Willenbrecht, F. F. Giguel, A. M. Tsibris, D. R. Kuritzkes, U. Demirci, *Small* **2013**, *9*, 2553.
- [178] a) A. Mokhtarzadeh, R. Eivazzadeh-Keihan, P. Pashazadeh, M. Hejazi, N. Gharaatifar, M. Hasanzadeh, B. Baradaran, M. de la Guardia, *TrAC, Trends Anal. Chem.* **2017**, *97*, 445; b) A. Bolotsky, D. Butler, C. Dong, K. Gerace, N. R. Glavin, C. Muratore, J. A. Robinson, A. Ebrahimi, *ACS Nano* **2019**, *13*, 9781.
- [179] L. Krejcová, L. Nejdil, M. A. M. Rodrigo, M. Zurek, M. Matousek, D. Hynek, O. Zitka, P. Kopel, V. Adam, R. Kizek, *Biosens. Bioelectron.* **2014**, *54*, 421.
- [180] S. Tsuda, L. A. Fraser, S. Sharabi, M. Hezwani, A. Kinghorn, S. Liang, G. Douce, J. Tanner, L. Cronin, *ChemRxiv* **2019**, <https://doi.org/10.26434/chemrxiv.7640414.v1>.

- [181] C. Park, J. Lee, Y. Kim, J. Kim, J. Lee, S. Park, *J. Microbiol. Methods* **2017**, *132*, 128.
- [182] K. S. Kumar, P.-Y. Chen, H. Ren, *Research* **2019**, *2019*, 3018568.
- [183] S. Zhao, R. Zhu, *Adv. Mater.* **2017**, *29*, 1606151.
- [184] Q. Hua, J. Sun, H. Liu, R. Bao, R. Yu, J. Zhai, C. Pan, Z. L. Wang, *Nat. Commun.* **2018**, *9*, 244.
- [185] A. Mohammadi, J. Lavranos, H. Zhou, R. Mutlu, G. Alici, Y. Tan, P. Choong, D. Oetomo, *PLoS One* **2020**, *15*, e0232766.
- [186] J. Muth, D. Vogt, R. Truby, *Adv. Mater.* **2014**, *26*, 6307.
- [187] C. Antfolk, M. D'alonzo, B. Rosén, G. Lundborg, F. Sebelius, C. Cipriani, *Expert Rev. Med. Devices* **2013**, *10*, 45.
- [188] J. H. Low, W. W. Lee, P. M. Khin, N. V. Thakor, S. L. Kukreja, H. L. Ren, C. H. Yeow, *IEEE Robot. Autom. Lett.* **2017**, *2*, 880.
- [189] M. O. Martinez, T. K. Morimoto, A. T. Taylor, A. C. Barron, J. A. Pultorak, J. Wang, A. Calasanz-Kaiser, R. L. Davis, P. Blikstein, A. M. Okamura, presented at *2016 IEEE Haptics Symp. (HAPTICS)*, IEEE, Philadelphia, PA **2016**.
- [190] F. D'Agnano, C. Balletti, F. Guerra, P. Vernier, *Int. Arch. Photogramm., Remote Sen. Spat. Inf. Sci.* **2015**, *40*, 207.
- [191] K. Kim, J. Park, J.-h. Suh, M. Kim, Y. Jeong, I. Park, *Sens. Actuators, A* **2017**, *263*, 493.
- [192] M. Nabeel, K. Aqeel, M. N. Ashraf, M. I. Awan, M. Khurram, presented at *2016 2nd Int. Conf. on Robotics and Artificial Intelligence (ICRAI)*, IEEE, Rawalpindi, Pakistan **2016**.
- [193] a) M. H. Ali, S. Batai, D. Sarbassov, *Rapid Prototyping J.* **2019**, *25*, 1108; b) M. Jiménez, L. Romero, I. A. Domínguez, M. d. M. Espinosa, M. Domínguez, *Complexity* **2019**, *2019*, 9656938.
- [194] Y. Oh, V. Bharambe, B. Mummareddy, J. Martin, J. McKnight, M. A. Abraham, J. M. Walker, K. Rogers, B. Conner, P. Cortes, E. MacDonald, J. J. Adams, *Addit. Manuf.* **2019**, *27*, 586.
- [195] M. A. Haque, N. McFarlane, N. V. Lavrik, D. Hensley, presented at *2019 30th Annual SEMI Advanced Semiconductor Manufacturing Conf. (ASMC)*, IEEE, Saratoga Springs, NY **2019**.
- [196] G. Ercolano, T. Zambelli, C. van Nisselroy, D. Momotenko, J. Vörös, T. Merle, W. W. Koelmans, *Adv. Eng. Mater.* **2020**, *22*, 1900961.
- [197] W. Gao, Y. Zhang, D. Ramanujan, K. Ramani, Y. Chen, C. B. Williams, C. C. L. Wang, Y. C. Shin, S. Zhang, P. D. Zavattieri, *Comput. -Aided Des.* **2015**, *69*, 65.
- [198] a) D. Z. Tansel, J. Brenneman, G. K. Fedder, R. Panat, J. *Micromech. Microeng.* **2020**, *30*, 067001; b) I. Gibson, D. Rosen, B. Stucker, M. Khorasani, in *Additive Manufacturing Technologies*, Springer, New York **2021**, p. 379.
- [199] a) V. Katseli, A. Economou, C. Kokkinos, *Electrochem. Commun.* **2019**, *103*, 100; b) K. Kadimisetty, J. Song, A. M. Doto, Y. Hwang, J. Peng, M. G. Mauk, F. D. Bushman, R. Gross, J. N. Jarvis, C. Liu, *Biosens. Bioelectron.* **2018**, *109*, 156.
- [200] V. Gambardella, N. Tarazona, J. M. Cejalvo, P. Lombardi, M. Huerta, S. Roselló, T. Fleitas, D. Roda, A. Cervantes, *Cancers* **2020**, *12*, 1009.



**Md. Azahar Ali** is a postdoc in the Department of Mechanical Engineering at Carnegie Mellon University. His current research focuses on 3D printed biosensors for pathogens and biomarker sensing. Earlier, he was a post-doc in the department of Electrical and Computer Engineering at Iowa State University. He obtained his Ph.D. degree from the Indian Institute of Technology Hyderabad. He is actively engaged in the area of bioMEMS and 3D printed biosensors. Dr. Ali will join Virginia Tech, Blacksburg, VA, as an Assistant Professor of Animal and Poultry Sciences in spring 2022.



**Chunshan Hu** is a Ph.D. candidate in the Department of Mechanical Engineering at Carnegie Mellon University. He received his BS degree from Northwest A&F University and M.S. degree in Mechanical Engineering from Washington State University. His research interests mainly focus on additive manufacturing of various nanoparticle-based materials including metals, ceramics, and polymers.



**Eric A. Yttri** is Eberly Family Career Development Professor of Biological Science at Carnegie Mellon University. Previously, he was a postdoctoral associate at Janelia Research Campus-HHMI after receiving his Ph.D. at Washington University in St. Louis and studying neuroscience at the College of William and Mary. Dr. Yttri's work employs technique development to further his research goals in basal ganglia function and brain-wide dynamics. He is the recipient of several awards, including from the Whitehall and Brain Research Foundations, the Whitehall, Kaufman, and Brain Research and is the current co-chair of the Allen Institute Next Generation Leaders Council.



**Rahul Panat** is Russell V. Trader Associate Professor of Mechanical Engineering and the Associate Director of the Manufacturing Futures Institute at Carnegie Mellon University. He received his M.S. in Mechanical Engineering from University of Massachusetts, Amherst, and his Ph.D. in Theoretical and Applied Mechanics from University of Illinois at Urbana-Champaign. After his Ph.D., he worked at Intel Corporation, Chandler, AZ, for a decade. Dr. Panat joined Washington State University, Pullman, before moving to CMU in 2017. He is the recipient of several awards such as Russell V. Trader Career Development Professorship (an Endowed Chair Professorship) at Carnegie Mellon, Materials Research Society gold medal, Henry L. Langhaar award and Mavis memorial fund award.